

VARYING TETHER LENGTHS  
FOR MODIFYING ORBITAL ECCENTRICITIES

by

SARAH A. GAVIT

B.S., Massachusetts Institute of Technology  
(1983)

SUBMITTED IN PARTIAL FULFILLMENT  
OF THE REQUIREMENTS OF THE  
DEGREE OF

MASTER OF SCIENCE

IN AERONAUTICAL AND ASTRONAUTICAL ENGINEERING

at the

MASSACHUSETTS INSTITUTE OF TECHNOLOGY

January 18, 1985

© Massachusetts Institute of Technology 1985

Signature of Author \_\_\_\_\_  
Department of Aeronautics and Astronautics

Certified by \_\_\_\_\_  
Professor Manuel Martinez-Sanchez  
Thesis Supervisor

Accepted by \_\_\_\_\_  
Professor Harold Y. Wachman  
Chairman, Departmental Graduate Committee

ARCHIVES

MASSACHUSETTS INSTITUTE  
OF TECHNOLOGY

FEB 14 1985

LIBRARIES

VARYING TETHER LENGTHS  
FOR MODIFYING ORBITAL ECCENTRICITIES

by

SARAH A. GAVIT

Submitted to the Department of  
Aeronautics and Astronautics on January 18, 1985  
in partial fulfillment of the requirements for  
the degree of Master of Science.

ABSTRACT

The purpose of this thesis was to derive linearized equations describing the variations in the orbital parameters resulting from the resonance between a periodically length varying tether system and its orbital frequency. A controlled periodic tether variation was assumed, from which the corresponding tether libration angle history was derived. This allowed the calculation of the radial and tangential accelerations acting on the tether system, and thus the changes in the orbital elements using the variational equations. The theoretical variations in the orbital elements were then compared to the results obtained by numerically integrating the equations of motion, with favorable results. The numerical analysis was extended to investigate cases not covered by the theory, as well as the tether tension profile and power requirements of the system.

Thesis Supervisor: Manuel Martinez-Sanchez  
Title: Associate Professor of Aeronautical  
and Astronautical Engineering

## ACKNOWLEDGEMENTS

First of all, I'd like to thank Martin Marietta Corporation for funding my thesis, an act they may regret as they put up with me for the next several years as a real employee.

Second, I would like to thank Professor Manuel Martinez-Sanchez. Of all the professors I've met, I've never met one I'd rather work for, or that is more patient. I think Dan Heimerdinger put it well in the acknowledgements of his master's thesis when he said, " thanks for letting me take the credit for all your work ".

Speaking of Dan Heimerdinger, and Dan Cousins for that matter, I'd like to thank them for helping me keep some form of sanity over the years. The SSL as a whole, especially Gerge Sarver, should be acknowledged for bearing with my growing pains at this wonderful place appropriately named the "institution". Special thanks to Professor Dave Akin and Javier DeLuis for helping in the production of this thesis.

Finally, I'd like to thank Professor Rene Miller, to whom I dedicate my thesis. His constant optimism and encouragement has helped me through many difficult times in the last six years.

## Table of Contents

	<u>Page</u>
I. INTRODUCTION	5
II. THEORETICAL ANALYSIS	12
2.1 The Equations of Motion	12
2.2 Solving for the Tether Libration Angle Given a Controlled Tether Length Variation	12
2.3 Determining the Average Change in the Orbital Elements Using the Variational Equations	32
III. THEORETICAL ANALYSIS vs. NUMERICAL ANALYSIS	42
3.1 Decreasing Orbital Eccentricity Using a Sine Variation of the Tether Length	44
3.2 Increasing Orbital Eccentricity Using a Sine Variation of the Tether Length	48
3.3 Constant Orbital Eccentricity Using a Cosine Variation of the Tether Length	49
IV. CONCLUSION	51
REFERENCES	53
FIGURES AND GRAPHS	54
APPENDIX A: Conservation of Angular Momentum for a Dumbbell in Orbit About a Spherical Planet	74
APPENDIX B: Derivation of the Tension in a Length Varying Tether	78
APPENDIX C: Numerical Analysis Program	82

## I. Introduction

Tsiolkovsky, a Russian, first considered the use of two masses connected by a string in tension, for exploiting weak gravity gradient forces in space in 1895.(1) It was not until the 1960's, that V.V Beletskii, also a Russian, suggested that a tether system whose length varied at the orbital frequency, could induce a resonance, which could be used for maneuvering space vehicles.(2) In 1968, V.V Beletskii and M.E. Givertz wrote, "it is possible to control the geometry of a body such that variations which occur in the force of gravity over time lead to substantial deviations in the body's trajectory from the original".(3) Investigation into the use of tethers for this purpose was not pursued, however, since tether lengths of tens to hundreds of kilometers would have to be used to produce significant accelerations of a tether system. Not until the 1970's with the development of new lightweight synthetic fibers, such as Kevlar, were practical applications of tethers seriously considered.

A varying length tether system may be envisioned as a dumbbell, two masses connected by a tether, whose length is made to vary via a powered winch located at one or both of the masses. The reeling in and out of the tether, often referred to as tether "pumping", sets up Coriolis forces

which induce in plane librations of the tether system about its center of mass. If the reeling operation is driven such that a resonance occurs with the orbital frequency, it is possible to change the energy of the orbit, and thus the trajectory of the tether system. Total angular momentum must remain constant, however, since the external forces are all central (if the attracting body is assumed spherical). This is proved in Appendix I.

In 1983, Manuel Martinez-Sanchez, professor of aeronautical and astronautical engineering at M.I.T., was the first to attempt quantifying possible orbital variations of spacecraft using length varying tethers.(4) His original paper contained several errors, which have since then been revised but not formally published. The equations in this section represent his corrected results (to be published, together with the higher order results of this work).

Martinez's preliminary analysis considered second order resonance effects in  $\ell/R$ , tether length over orbital radius, but only first order effects in  $\alpha$ , the tether libration angle, for near circular orbits. For simplicity of calculations, the tether libration angle,  $\alpha$ , was assumed to vary sinusoidally with constant amplitude. With this restriction, an equation for the tether length as a function of orbital position was derived from the equations of

motion. The tether libration angle and tether length were given by

$$\alpha = \alpha_0 \sin(\Omega t) \quad (1.1)$$

$$\ell = \bar{\ell} \{1 + \alpha_0 \cos(\Omega t)\} \quad (1.2)$$

where,

$\Omega$  = orbital frequency

$\alpha$  = libration angle amplitude

$\bar{\ell}$  = mean tether length

An illustration of the variations in the tether libration angle and length over one orbit are illustrated in Figure I.

The equations of motion were given by:

$$m(\ddot{R} - R\dot{\theta}^2) = \frac{-\mu m}{R^2} - \frac{3\mu m_{12}}{R^2} \left(\frac{\ell}{R}\right)^2 \left[1 - \frac{3}{2} \sin^2 \alpha\right]$$

$$m \frac{d}{dt}(R^2 \dot{\theta}) = \frac{3\mu}{R} m_{12} \left(\frac{\ell}{R}\right)^2 \sin \alpha \cos \alpha$$

$$mR^2 \ddot{\theta} + m_{12} \ell^2 (\ddot{\alpha} + \dot{\theta}) = L$$

where,

- $m_1$  = mass of the weight on the lower end of the tether  
 $m_2$  = mass of the weight on the upper end of the tether  
 $m_{12} = \frac{m_1 m_2}{m_1 + m_2}$   
 $\mu$  = earth's gravitational constant  
 $R$  = center of mass orbital radius (measured from the center of the earth)  
 $\theta$  = true anomaly

Equations (3) and (4) describe the conservation of the radial and tangential momentum of the tether system.

Equation (5) expresses conservation of total angular momentum which is the sum of the angular momentum of the center of mass, and the angular momentum of the tether system about its center of mass.

After perturbing the equations of motion, several useful first order approximations of the changes in apogee radius,  $R_a$ , perigee radius,  $R_p$ , and orbital eccentricity,  $e$ , were found as a function of the number of orbits over which the tether length had been perturbed,  $N$ .

$$R_a = R + 6 \frac{m_{12}}{m} \frac{\bar{l}^2}{R} \alpha_0 \left( \frac{3}{2} + 2N \right) \pi \quad (1.6)$$

$$R_p = R - 6 \frac{m_{12}}{m} \frac{\bar{l}^2}{R} \alpha_0 \left( \frac{1}{2} + 2N \right) \pi \quad (1.7)$$



$$e = 12N\pi \frac{m_{12}}{m} \left(\frac{\bar{\ell}}{R}\right)^2 \alpha_0 . \quad (1.8)$$

Successive apogee passages were found to be increasingly higher, developing  $90^\circ$  past  $\theta = 0.0$  (the point of maximum tether length), while successive perigee passages were found to be increasingly lower, developing  $270^\circ$  past  $\theta = 0.0$ . The semimajor axis,  $a$ , and the orbital energy,  $E$ , were found to be constant to first order. Calculation of a possible rotation of the argument of pericenter,  $\omega$ , was not attempted.

As an example, for a tether system with a center of mass radius of 6770 km, a mean tether length of 100 km, a lower mass of 100,000 kg, an upper mass of 10,000 kg, and a libration amplitude of .2 radians, the apogee will increase and the perigee will decrease by approximately 1.6 km/orbit, or, after one month, a circular orbit can develop to an orbit with eccentricity  $e = .064$ .

Martinez's analysis demonstrated that the first order variation in orbital eccentricity using a length varying tether was substantial enough to warrant further investigation into higher order perturbation effects of the orbital elements, as well as possible applications of this

orbital resonance technique.

The purpose of this thesis is to calculate the second order variations in libration angle and orbital eccentricity, of the orbital elements due to tether orbital resonance. Averaging these variations will result in an "ironed out" means of obtaining the changes in the orbital elements over an extended period of time. Of particular interest, will be the variations in the semimajor axis which had not been found in Martinez's first order analysis, and the rotation of the argument of perihelion, which was not accounted for. This paper will also extend the theory to include higher eccentric orbits.

Contrary to the former technique of picking a sinusoidal libration angle and then solving for a corresponding tether length variation, this analysis will select a simple tether length variation and solve for the natural angle of tether libration that results. This technique is considerably more difficult analytically, but seems more reasonable for practical applications, since it is easier to control tether length than tether angle. In fact, it may be impossible with only finite length control to impose an arbitrary libration time history against the combined action of natural gravity gradient oscillations and those imposed by orbital eccentricity.

Finally, possible applications of the tether orbital resonance technique will be considered. Orbital variations predicted by the second order perturbation theory will be compared to numerical results obtained by directly integrating the equations of motion. The numerical analysis will also be extended to include several cases not covered by the perturbation theory.

## II. Theoretical Analysis

The following sections derive the second order variations in  $l/R$ ,  $e$ , and  $\alpha$ , of the orbital elements that result from forced resonance between a length varying tether system and its orbital frequency. First Martinez's derivation of the equations of motion of a dumbbell in orbit is briefly summarized in Section 2.1. Section 2.2 discusses a method for finding the tether libration angle as a function of orbital position, given a controlled tether length variation. This allows the calculation of the disturbing radial and tangential accelerations which act on the tether system in Section 2.3, which in turn yields the perturbation terms in the variational equations of the orbital elements. Finally, these equations are averaged to find the mean values of the orbital elements as a function of orbital position and time.

### 2.1 The Equations of Motion

Consider a body orbiting about its center of attraction at  $O$ . See Figure 2. The distance from  $O$  to the center of mass, c.m., is given by the parameter  $R$ , while the distance from  $O$  to a point mass in the body,  $P$ , is given by the parameter  $R'$ . Newton's differential equation for the two

body' problem is,

$$\frac{d^2 \bar{R}}{dt^2} + \frac{\mu}{R^3} \bar{R} = 0 \quad (2.1)$$

Using this equation and the geometry in Figure 2, the point mass radial and tangential gravitational accelerations may be described by the following equations:

$$a_r = \frac{-\mu}{(R')^2} \cos \Delta \theta \quad (2.2)$$

$$a_\theta = \frac{-\mu}{(R')^2} \sin \Delta \theta \quad (2.3)$$

$R'$  and  $\ell/(R)^2$  are given to second order in  $x/R$  as follows:

$$\bar{R}' = x \bar{i}_x + (R+y) \bar{i}_y \quad (2.4)$$

$$\frac{1}{(R')^2} \approx \frac{1}{R^2} \left[ 1 - 2 \frac{y}{R} + \frac{3y^2 - x^2}{R^2} \right] \quad (2.5)$$

For small changes in  $\theta$ ,  $\cos(\Delta\theta)$  and  $\sin(\Delta\theta)$  may be approximated by their series expansions.

$$\cos \Delta \theta \approx 1 - 1/2 \left( \frac{x}{R} \right)^2 \quad (2.6)$$

$$\sin\Delta\theta \approx \frac{x}{R} - \frac{xy}{R^2} \quad (2.7)$$

Substituting equations (2.5), (2.6); and (2.7) into equations (2.2) and (2.3), one obtains the second order approximations in  $x/R$  of the radial and tangential gravitational accelerations:

$$a_r = \frac{-\mu}{R} \left[ 1 - 2 \frac{y}{R} + 3 \frac{y^2 - 1/2 x^2}{R^2} \right] \quad (2.8)$$

$$a_\theta = \frac{-\mu}{R^2} \frac{x}{R} \left[ 1 - 2 \frac{y}{R} \right] \quad (2.9)$$

The sum of the forces acting per unit mass on all point masses in the body may then be equated to the radial and tangential accelerations of the center of mass.

$$m(\ddot{R} - \dot{\theta}^2 R) = \frac{-\mu m}{R^2} - \frac{3\mu}{R^4} \left[ \sum_i m_i y_i^2 - 1/2 \sum_i m_i x_i^2 \right] \quad (2.10)$$

$$\frac{m}{R} \frac{d}{dt} [R^2 \dot{\theta}] = \frac{3\mu}{R^4} \sum_i m_i x_i y_i \quad (2.11)$$

Finally, total angular momentum about the attracting center may be written as the sum of the angular momentum of the center of mass about the center of attraction, and the

angular momentum of the point masses about the center of mass.

$$mR^2\dot{\theta} + \left[ \sum_i m_i (x_i^2 + y_i^2) \right] (\dot{\alpha} + \dot{\theta}) = L = \text{const} \quad (2.12)$$

Equations (2.10), (2.11), and (2.12) may now be specialized to describe an orbiting body with a dumbbell configuration. Using the geometry of Figure 3, one may write the following equations:

$$\sum_i m_i x_i^2 = m_1 x_1^2 + m_2 x_2^2 = m_{12} \ell^2 \sin^2 \alpha \quad (2.13)$$

$$\sum_i m_i y_i^2 = m_1 y_1^2 + m_2 y_2^2 = m_{12} \ell^2 \cos^2 \alpha \quad (2.14)$$

$$\sum_i m_i x_i y_i = m_1 x_1 y_1 + m_2 x_2 y_2 = m_{12} \ell^2 \sin \alpha \cos \alpha \quad (2.15)$$

where,

$$m = m_1 + m_2 \quad (2.16)$$

$$m_{12} = \frac{m_1 m_2}{m} \quad (2.17)$$

Substituting equations (2.13), (2.14), and (2.15), into equations (2.10), (2.11) and (2.12), the equations of motion may be written as follows:

$$m(\ddot{R} - R\dot{\theta}^2) = \frac{-\mu m}{R^2} - \frac{3\mu m_{12}}{R^2} \left(\frac{l}{R}\right)^2 \left[1 - \frac{3}{2} \sin^2 \alpha\right] \quad (2.18)$$

$$m \frac{d}{dt}(R^2 \dot{\theta}) = \frac{3\mu}{R} m_{12} \left(\frac{l}{R}\right)^2 \sin \alpha \cos \alpha \quad (2.19)$$

$$mR^2 \dot{\theta} + m_{12} l^2 (\dot{\alpha} + \dot{\theta}) = L \quad (2.20)$$

Combining equations (2.19) and (2.20), results in the useful gravity gradient oscillation equation.

$$\frac{d}{dt} [L^2 (\dot{\alpha} + \dot{\theta})] = \frac{-3\mu}{R} \left(\frac{l}{R}\right)^2 \sin \alpha \cos \alpha \quad (2.21)$$

## 2.2 Solving for the Tether Libration Angle given a Controlled Tether Length Variation

In this section, the libration angle,  $\alpha$ , will be determined as a function of orbital position using the gravity gradient oscillation equation, (2.21).

First, solving for  $\dot{\theta}$  from equation (2.20) and linearizing to second order in  $l/R$ , one finds,

$$\dot{\theta} = \frac{h}{R^2} \left[1 - \frac{m_{12}}{m} \left(\frac{l}{R}\right)^2 \left(\frac{d\alpha}{d\theta} + 1\right)\right] \quad (2.22)$$



This equation may be used to rewrite the oscillation equation, (2.21), in terms of  $\theta$  as follows:

$$\frac{d}{d\theta} \left[ \left( \frac{\ell}{R} \right)^2 \left( 1 + \frac{d\alpha}{d\theta} \right) \right] = \frac{-3\mu}{h^2} \frac{\ell^2}{R} \sin\alpha \cos\alpha \quad (2.23)$$

Notice that the form  $\dot{\theta} \approx h/R^2$  of equation (2.22) has been used, since the right hand side of equation (2.21) is itself already of second order in  $\ell/R$ . Now, assume a tether length control law, (2.24), and near Keplarian motion over one orbit, (2.25). The latter approximation results from the fact that tether-induced perturbations of the center of mass orbit are also quadratic in  $\ell/R$ , and would only introduce higher order libration perturbations through equation (2.21).

$$\ell = \bar{\ell} (1 + \lambda_c \cos\theta + \lambda_s \sin\theta) \quad (2.24)$$

$$R = \frac{p}{1 + e \cos\theta} \quad (2.25)$$

For perturbation analysis, the orders of smallness of  $e$ , and  $\alpha$  are not independent, because, even without length variations, the tether will librate due to the orbital eccentricity with an amplitude approximately equal to  $e$ . Similarly, libration angles due to length variation are of the order of  $\lambda_c$ ,  $\lambda_s$ . We here retain up to and including quadratic terms in  $e$ ,  $\alpha$ ,  $\lambda_c$  and  $\lambda_s$ . Notice that this is the

highest order which still makes the problem linear in  $\alpha$   
 $(\sin\alpha \cos\alpha \approx \alpha + O(\alpha^3))$ .

Expanding equation (2.23) to this order gives the result

$$\frac{d}{d\theta} \left[ F(\theta) \frac{d\alpha}{d\theta} \right] + 3G(\theta) \alpha = H(\theta) \quad (2.26)$$

which can be recognized as a linear, second order,  
 inhomogeneous, differential equation for  $\alpha$  with respect to  
 the independent variable  $\theta$ . Here we have

$$F(\theta) = 1 + 2(e + \lambda_c) \cos\theta + 2\lambda_s \sin\theta \quad (2.27)$$

$$G(\theta) = 1 + (e + 2\lambda_c) \cos\theta + 2\lambda_s \sin\theta \quad (2.28)$$

$$\begin{aligned} H(\theta) &= 2(e + \lambda_c) \sin\theta - 2\lambda_s \cos\theta \\ &\quad - (4\lambda_s e + 2\lambda_s \lambda_c) (\cos^2\theta - \sin^2\theta) \\ &\quad + 2(e^2 + 4\lambda_c e + \lambda_c^2 - \lambda_s^2) \sin\theta \cos\theta \end{aligned} \quad (2.29)$$

It can be seen that the equation has periodic coefficients in  
 $\theta$ . Expanding the derivative term in (2.26) and dividing by  
 $F(\theta)$  one obtains,

$$\frac{d^2 \alpha}{d\theta^2} + \frac{d\alpha}{d\theta} \frac{F_\theta}{F} + \frac{3G(\theta)}{F} \alpha = \frac{H(\theta)}{F} \quad (2.30)$$

$F(\theta)$  is now written as  $F$ , and  $F_\theta$  and  $F_{\theta\theta}$  represent the first and second derivatives of  $F$ . Using the transformation,

$$\alpha = e^{-1/2 \int \frac{F_\theta}{F} d\theta} U = \frac{U}{\sqrt{F}} \quad (2.31)$$

gives an equation with no first derivative term:

$$U_{\theta\theta} + U \left[ \frac{1/4 F_\theta^2 - 1/2 F_{\theta\theta} F}{F^2} + \frac{3G}{F} \right] = \frac{H(\theta)}{\sqrt{F}} \quad (2.32)$$

Using equations (2.27), (2.28) and (2.29), to expand the coefficients of (2.32) to second order in  $e$ ,  $\lambda_c$  and  $\lambda_s$ , one obtains the following result:

$$\begin{aligned} U_{\theta\theta} + U[3 + (\lambda_c - 2e) \cos\theta + \lambda_s \sin\theta] \\ = 2(e + \lambda_c) \sin\theta - 2\lambda_s \cos\theta \\ + 4\lambda_c e \cos\theta \sin\theta + 2\lambda_s e (\sin^2\theta - \cos^2\theta) \end{aligned} \quad (2.33)$$

This equation may be rewritten as

$$\begin{aligned}
U_{\theta\theta} + U [3 - \sqrt{\lambda_s^2 + (2e - \lambda_c)^2} \cos\beta] \\
= 2(e + \lambda_c)\sin\theta - 2\lambda_s\cos\theta + 4\lambda_c e\cos\theta\sin\theta \\
+ 2\lambda_s e (\sin^2\theta - \cos^2\theta)
\end{aligned} \tag{2.34}$$

where,

$$\beta = \theta + \tan^{-1} \left[ \frac{\lambda_s}{2e - \lambda_c} \right] \tag{2.35}$$

Now, define  $\phi$  to be,

$$\phi = 1/2 \beta \tag{2.36}$$

Transforming equation (2.34) into  $\phi$  coordinates gives the following second order differential equation with nonconstant coefficients, easily recognized as Mathieu's equation.

$$\begin{aligned}
U_{\phi\phi} + U [12 + 4\sqrt{\lambda_s^2 + (2e - \lambda_c)^2} - 8\sqrt{\lambda_s^2 + (2e - \lambda_c)^2} \cos^2\phi] \\
= 8 [(e + \lambda_c)\sin\theta - \lambda_s\cos\theta + 2\lambda_c e\cos\theta\sin\theta \\
+ \lambda_s e (\sin^2\theta - \cos^2\theta)]
\end{aligned} \tag{2.37}$$

The solution to this equation, along with equation (2.31) will yield the desired expression for the libration angle,  $\alpha$ , as a function of orbital position.

First, a homogeneous solution to equation (2.37) will be found using the techniques for solving Mathieu's equation in Reference 5.

Let parameters  $b$  and  $h$  be described by the following equations:

$$b = 12 + 4 \sqrt{\lambda_s^2 + (2e - \lambda_c)^2} \quad (2.38)$$

$$h^2 = 8 \sqrt{\lambda_s^2 + (2e - \lambda_c)^2} \quad (2.39)$$

According to Figure 4, equation (2.37) falls well within the stable region for Mathieu's equation. Thus, (2.37) has two homogeneous solutions, one even and one odd, neither of which is periodic in  $\phi$ . These solutions truncated at the level which is consistent with second-order accuracy in  $e$ ,  $\lambda_c$ , and  $\lambda_s$ , are given by,

$$\begin{aligned} S_e(b, h; z) &= \sum_{n=-\infty}^{\infty} a_n \text{Cos} [(S + 2n)\phi] \\ &\approx a_{-2} \text{Cos} [(S - 4)\phi] + a_{-1} \text{Cos} [(S - 2)\phi] \\ &+ a_0 \text{Cos} [S\phi] + a_1 \text{Cos} [(S + 2)\phi] \\ &+ a_2 \text{Cos} [(S + 4)\phi] \end{aligned} \quad (2.40)$$

$$\begin{aligned}
S_0(b, h; z) &= \sum_{n=-\infty}^{\infty} a_n \sin[(S + 2n)\phi] \\
&= a_{-2} \sin[(S - 4)\phi] + a_{-1} \sin[(S - 2)\phi] \\
&\quad + a_0 \sin[S\theta] + a_1 \sin[(S + 2)\theta] \\
&\quad + a_2 \sin[(S + 4)\phi]
\end{aligned} \tag{2.41}$$

where, using

$$z = \cos \phi \tag{2.42}$$

$$\begin{aligned}
s &= \sqrt{b} \left[ 1 - \frac{h^2}{4b} - \frac{h^4}{64b^2} \left( \frac{2 - 3b}{1 - b} \right) \right] \\
&\approx \sqrt{12} \left[ 1 - \frac{h^4}{8448} \right]
\end{aligned} \tag{2.43}$$

gives,

$$a_0 = 1 \tag{2.44}$$

$$\begin{aligned}
a_1 &= \frac{-h^2}{16(1 + S/2)^2 + 2h^2 - 4b - h^4(\dots)} \\
&\approx \frac{-h^2}{16(1 + 2\sqrt{3})}
\end{aligned} \tag{2.45}$$

$$a_2 = \frac{-a_1 h^2}{16(S/2+2)^2 + 2h^2 - 4b - h^4 (\dots)}$$

$$\approx \frac{h^4}{1024(7 + 3\sqrt{3})} \quad (2.46)$$

$$a_{-1} = \frac{-h^2}{16(1 - S/2)^2 + 2h^2 - 4b - h^4 (\dots)}$$

$$\approx \frac{-h^2}{16(1 - 2\sqrt{3})} \quad (2.47)$$

$$a_{-2} = \frac{-a_{-1} h^2}{16(S/2 - 2)^2 + 2h^2 - 4b + h^4 (\dots)}$$

$$\approx \frac{h^4}{1024(7 - 3\sqrt{3})} \quad (2.48)$$

Substituting equations (2.43) through (2.48) into equations (2.40) and (2.41) one obtains,

$$S_e = \text{Cos}[\sqrt{12} (1 - \frac{h^4}{8448})\phi] + \frac{h^4}{1024} \left[ \frac{\text{Cos}(\sqrt{12} - 4)\phi}{(7 - 3\sqrt{3})} + \frac{\text{Cos}(\sqrt{12} + 4)\phi}{(7 + 3\sqrt{3})} \right]$$

$$- \frac{h^2}{16} \left[ \frac{\text{Cos}(\sqrt{12} - 2)\phi}{(1 - 2\sqrt{3})} + \frac{\text{Cos}(\sqrt{12} + 2)\phi}{(1 + 2\sqrt{3})} \right] \quad (2.49)$$

$$\begin{aligned}
S_o = & \sin \left[ \sqrt{12} \left( 1 - \frac{h^4}{8448} \right) \phi \right] + \frac{h^4}{1024} \left[ \frac{\sin(\sqrt{12} - 4)\phi}{(7 - 3\sqrt{3})} + \frac{\sin(\sqrt{12} + 4)\phi}{(7 + 3\sqrt{3})} \right. \\
& \left. - \frac{h^2}{16} \left[ \frac{\sin(\sqrt{12} - 2)\phi}{(1 - 2\sqrt{3})} + \frac{\sin(\sqrt{12} + 2)\phi}{(1 + 2\sqrt{3})} \right] \right] \quad (2.50)
\end{aligned}$$

Define  $\phi$  and  $\lambda$  to be the following:

$$\phi = 1/2 (\theta + \lambda) \quad (2.51)$$

$$\lambda = \tan^{-1} \left[ \frac{\lambda_s}{2e^{-\lambda_c}} \right] \quad (2.52)$$

To calculate the particular solution of equation (2.37), only the first order terms in  $e$ ,  $\lambda_c$  and  $\lambda_s$ , of the homogeneous solutions, (2.49) and (2.50), are required, since the forcing term in (2.37) is of first or higher order itself. Therefore, using equations (2.51) and (2.52), the homogeneous solutions (up to arbitrary multiplicative constants) may be written to first order as ,

$$\begin{aligned}
S_e = & \cos \sqrt{3}(\theta + \lambda) - \frac{h^2}{16} \left[ \frac{\cos(\sqrt{3} - 1)(\theta + \lambda)}{(1 - 2\sqrt{3})} \right. \\
& \left. + \frac{\cos(\sqrt{3} + 1)(\theta + \lambda)}{(1 + 2\sqrt{3})} \right] \quad (2.53)
\end{aligned}$$



$$\begin{aligned}
S_o = \sin \sqrt{3}(\theta + \lambda) - \frac{h^2}{16} & \left[ \frac{\sin(\sqrt{3} - 1)(\theta + \lambda)}{(1 - 2\sqrt{3})} \right. \\
& \left. + \frac{\sin(\sqrt{3} + 1)(\theta + \lambda)}{(1 + 2\sqrt{3})} \right]
\end{aligned} \tag{2.54}$$

The particular solution of equation (2.37) will be determined below by variation of parameters as described in Reference 6. For our case, the particular solution is given as follows:

$$y = \frac{1}{W} \int_0^\phi Q(\xi) [S_e(\xi)S_o(\phi) - S_o(\xi)S_e(\phi)] d\xi + C_1 S_e(\phi) + C_0 S_o(\phi) \tag{2.55}$$

where  $\xi$  is a dummy argument of integration,  $Q$  is the forcing term of equation (2.37), and  $W$  is the Wronskian given by,

$$W = S_e \left( \frac{dS_o}{d\phi} \right) - S_o \left( \frac{dS_e}{d\phi} \right) = 2\sqrt{3} \tag{2.56}$$

The Wronskian must be constant since the homogeneous part of equation (2.37) is of the form,

$$\frac{d^2 U}{d\phi^2} + r \frac{dU}{d\phi} = 0 \tag{2.57}$$

Substituting equations (2.53), (2.54) and (2.56) as well as the right hand side of equation (2.37) into equation (2.55), expanding to second order in  $e$ ,  $\lambda_c$  and  $\lambda_s$ , integrating, and collecting terms, one obtains the following second order particular solution:

$$\begin{aligned}
 Y_p = \frac{4}{\sqrt{3}} [ & C_1 \text{Cos}(\theta + \phi_1) + C_8 \text{Cos}(\sqrt{3}\theta + \phi_8) + C_{11} \text{Cos}(2\theta - \phi_{11}) \\
 & + C_{12} \text{Cos}(\lambda + \phi_{12}) + C_{15} \text{Cos}((\sqrt{3} - 1)\theta + \phi_{15}) \\
 & + C_{18} \text{Cos}((\sqrt{3} + 1)\theta + \phi_{18}) ] \tag{2.58}
 \end{aligned}$$

where,

$$K_1 = \sqrt{(e + \lambda_c)^2 + \lambda_s^2}$$

$$K_2 = \sqrt{\lambda_c^2 + \lambda_s^2}$$

$$C_1 = \frac{-\sqrt{3} K_1}{4}$$

$$C_2 = \frac{[528 - 352\sqrt{3} + h^2(20 - 8\sqrt{3})]}{6336 - 3520\sqrt{3}} K_1$$

$$C_3 = \frac{[528 + 352\sqrt{3} + h^2(20 + 8\sqrt{3})]}{-6336 - 3520\sqrt{3}} K_1$$

$$C_4 = \frac{eK_2}{-8 + 4\sqrt{3}}$$

$$C_5 = \frac{eK_2}{8 + 4\sqrt{3}}$$

$$C_6 = \sqrt{C_2^2 + C_3^2 + 2C_2C_3 \cos(\phi_2 - \phi_3)}$$

$$C_7 = \sqrt{C_4^2 + C_5^2 + 2C_4C_5 \cos(\phi_4 - \phi_5)}$$

$$C_8 = \sqrt{C_6^2 + C_7^2 + 2C_6C_7 \cos(\phi_6 - \phi_7)}$$

$$C_9 = \frac{\sqrt{3}e K_2}{2}$$

$$C_{10} = \frac{\sqrt{3}}{64} h^2 K_1$$

$$C_{11} = \sqrt{C_9^2 + C_{10}^2 + 2C_9C_{10} \cos(\phi_9 - \phi_{10})}$$

$$C_{12} = \frac{-h^2 K_1}{64\sqrt{3}}$$

$$C_{13} = \frac{h^2 K_1}{448 - 192\sqrt{3}}$$

$$C_{14} = \frac{h^2 K_1}{320 + 64\sqrt{3}}$$

$$C_{15} = \sqrt{C_{13}^2 + C_{14}^2 + 2C_{13}C_{14} \cos(\phi_{13} - \phi_{14})}$$

$$C_{16} = \frac{h^2 K_1}{-320 + 64\sqrt{3}}$$

$$C_{17} = \frac{-h^2 \sqrt{K_1}}{448 + 192\sqrt{3}}$$

$$C_{18} = \sqrt{C_{16}^2 + C_{17}^2 + 2C_{16}C_{17} \cos(\phi_{16} - \phi_{17})}$$

$$\psi_1 = \psi_2 = \psi_{10} = \psi_{13} = \psi_{16} = \tan^{-1} \left[ \frac{e + \lambda_c}{\lambda_s} \right]$$

$$\psi_3 = \psi_{12} = \psi_{14} = \psi_{17} = \tan^{-1} \left[ -\frac{e + \lambda_c}{\lambda_s} \right]$$

$$\psi_4 = \psi_9 = \tan^{-1} \left[ \frac{\lambda_c}{\lambda_s} \right]$$

$$\psi_5 = \tan^{-1} \left[ -\frac{\lambda_c}{\lambda_s} \right]$$

$$\phi_1 = \psi_1$$

$$\phi_2 = (\sqrt{3} - 1)\lambda + \psi_2$$

$$\phi_3 = (\sqrt{3} + 1)\lambda + \psi_3$$

$$\phi_4 = (\sqrt{3} - 2)\lambda + \psi_4$$

$$\phi_5 = (\sqrt{3} + 2)\lambda + \psi_5$$

$$\phi_6 = \tan^{-1} \left[ \frac{C_2 \sin \phi_2 + C_3 \sin \phi_3}{C_2 \cos \phi_2 + C_3 \cos \phi_3} \right]$$

$$\phi_7 = \tan^{-1} \left[ \frac{C_4 \sin \phi_4 + C_5 \sin \phi_5}{C_4 \cos \phi_4 + C_5 \cos \phi_5} \right]$$

$$\phi_8 = \tan^{-1} \left[ \frac{C_6 \sin \phi_6 + C_7 \sin \phi_7}{C_6 \cos \phi_6 + C_7 \cos \phi_7} \right]$$

$$\phi_9 = \psi_9$$

$$\phi_{10} = \lambda + \psi_{10}$$

$$\phi_{11} = \tan^{-1} \left[ \frac{C_9 \sin \phi_9 + C_{10} \sin \phi_{10}}{C_9 \cos \phi_9 + C_{10} \cos \phi_{10}} \right]$$

$$\phi_{12} = \psi_{12}$$

$$\phi_{13} = (\sqrt{3} - 2)\lambda + \psi_{13}$$

$$\phi_{14} = \sqrt{3} \lambda + \psi_{14}$$

$$\phi_{15} = \tan^{-1} \left[ \frac{C_{13} \sin \phi_{13} + C_{14} \sin \phi_{14}}{C_{13} \cos \phi_{13} + C_{14} \cos \phi_{14}} \right]$$

$$\phi_{16} = \sqrt{3} \lambda + \psi_{16}$$

$$\phi_{17} = (\sqrt{3} + 2)\lambda + \psi_{17}$$

$$\phi_{18} = \tan^{-1} \left[ \frac{C_{16} \sin \phi_{16} + C_{17} \sin \phi_{17}}{C_{16} \cos \phi_{16} + C_{17} \cos \phi_{17}} \right]$$

The complete solution of equation (2.37) is simply the sum of the homogeneous and particular solutions

$$U = S_e + S_o + Y_p \quad (2.59)$$

The constants A and B of the homogeneous solutions will henceforth be considered to be the same order as  $e$ ,  $\lambda_c$  and  $\lambda_s$ , which is permissible since A and B are simply determined by initial conditions on  $\alpha$  and  $\alpha_\theta$ , themselves presumably small.

By substituting (2.59) into (2.31), the libration angle,  $\alpha$ , may be determined as a function of orbital position, to second order in  $\ell/R$  as well as  $e$ ,  $\lambda_c$ ,  $\lambda_s$ , A and B.

$$\begin{aligned}
\alpha = & A \cos \sqrt{3}(\theta + \lambda) + B \sin \sqrt{3}(\theta + \lambda) + \frac{4}{\sqrt{3}} C_1 \cos(\theta + \phi_1) \\
& + \frac{4}{\sqrt{3}} C_8 \cos(\sqrt{3}\theta + \phi_8) - \frac{Ah^2}{16} \left[ \frac{\cos(\sqrt{3}-1)(\theta + \lambda)}{(1-2\sqrt{3})} + \frac{\cos(\sqrt{3}+1)(\theta + \lambda)}{(1+2\sqrt{3})} \right] \\
& - \frac{Bh^2}{16} \left[ \frac{\sin(\sqrt{3}-1)(\theta + \lambda)}{(1-2\sqrt{3})} + \frac{\sin(\sqrt{3}+1)(\theta + \lambda)}{(1+2\sqrt{3})} \right] \\
& + \frac{4}{\sqrt{3}} C_{11} \cos(2\theta + \phi_{11}) + \frac{4}{\sqrt{3}} C_{12} \cos(\lambda + \phi_{12}) \\
& + \frac{4}{\sqrt{3}} C_{15} \cos[(\sqrt{3}-1)\theta + \phi_{15}] + \frac{4}{\sqrt{3}} C_{18} \cos[(\sqrt{3}-1)\theta + \phi_{18}] \\
& - A(e + \lambda_c) \cos \theta \cos \sqrt{3}(\theta + \lambda) - B(e + \lambda_c) \cos \theta \sin \sqrt{3}(\theta + \lambda)
\end{aligned}$$

$$\begin{aligned}
& - \frac{4}{\sqrt{3}} C_1 (e + \lambda_c) \cos \theta \cos(\theta + \phi_1) - \frac{4}{\sqrt{3}} C_8 (e + \lambda_c) \cos \theta \cos(\sqrt{3}\theta + \phi_8) \\
& - A \lambda_s \sin \theta \cos \sqrt{3}(\theta + \lambda) - B \lambda_s \sin \theta \sin \sqrt{3}(\theta + \lambda) \\
& - \frac{4}{\sqrt{3}} C_1 \lambda_s \sin \theta \cos(\theta + \phi_1) - \frac{4}{\sqrt{3}} C_8 \lambda_s \sin \theta \cos(\sqrt{3}\theta + \phi_8) \tag{2.60}
\end{aligned}$$

### 2.3 Determining the Average Change in the Orbital Elements Using the Variational Equations

The derivation of the equation for the libration angle,  $\alpha$ , as a function of orbital position in Section 2.2, now permits the calculation of the radial and tangential acceleration acting on a tether system whose length varies periodically. According to equations (2.18) and (2.19), the perturbing radial and tangential accelerations acting on an orbiting dumbbell are given by,

$$a_r = \frac{-3\mu}{R^2} \frac{m_{12}}{m} \left(\frac{l}{R}\right)^2 \left(1 - \frac{3}{2} \sin^2 \alpha\right) \tag{2.61}$$

$$a_\theta = \frac{3\mu}{R^2} \frac{m_{12}}{m} \left(\frac{l}{R}\right)^2 \sin \alpha \cos \alpha \tag{2.62}$$



Assuming a small  $\alpha$  approximation, and substituting equations (2.24) and (2.60) into equations (2.61) and (2.62), one obtains the following approximations of the perturbing radial and tangential accelerations to second order in  $\mathcal{L}/R$  as well as in  $e$ ,  $\lambda_c$ ,  $\lambda_s$ ,  $A$  and  $B$ .

$$\begin{aligned}
a_r = & 3\mu \frac{m_{12}}{m} \frac{\bar{e}^2}{a} [-1 - (2\lambda_c + 4e)\cos\theta - 2\lambda_s \sin\theta \\
& + \frac{3}{2} A^2 \cos^2\sqrt{3}(\theta+\lambda) + 3ABC\cos\sqrt{3}(\theta+\lambda)\sin\sqrt{3}(\theta+\lambda) \\
& + \frac{12}{\sqrt{3}} AC_1 \cos\sqrt{3}(\theta+\lambda)\cos(\theta+\phi_1) \\
& + \frac{12}{\sqrt{3}} AC_8 \cos\sqrt{3}(\theta+\lambda)\cos(\sqrt{3}\theta+\phi_8) + \frac{3}{2} B^2 \sin^2\sqrt{3}(\theta+\lambda) \\
& + \frac{12}{\sqrt{3}} BC_1 \sin\sqrt{3}(\theta+\lambda)\cos(\theta+\phi_1) + \frac{12}{\sqrt{3}} BC_8 \sin\sqrt{3}(\theta+\lambda)\cos(\sqrt{3}\theta+\phi_8) \\
& + 16C_1 C_8 \cos(\theta+\phi_1)\cos(\sqrt{3}\theta+\phi_8) + 8C_1^2 \cos^2(\theta+\phi_1) \\
& + 8C_8^2 \cos^2(\sqrt{3}\theta+\phi_8) - (2\lambda_c \lambda_s + 8e\lambda_s)\sin\theta\cos\theta \\
& - (\lambda_c^2 + 8e\lambda_c + 6e^2)\cos^2\theta - \lambda_s^2 \sin^2\theta - 4e^2] \tag{2.63}
\end{aligned}$$

$$\begin{aligned}
a_{\theta} = & 3\mu \frac{m_{12}}{m} \frac{\bar{x}^2}{a} [A \cos \sqrt{3}(\theta + \lambda) + B \sin \sqrt{3}(\theta + \lambda) + \frac{4}{\sqrt{3}} C_1 \cos(\theta + \phi_1) \\
& + \frac{4}{\sqrt{3}} C_8 \cos(\sqrt{3}\theta + \phi_8) - \frac{Ah^2}{16} \frac{\cos(\sqrt{3}-1)(\theta + \lambda)}{(1-2\sqrt{3})} + \frac{\cos(\sqrt{3}+1)(\theta + \lambda)}{(1+2\sqrt{3})} \\
& - \frac{Bh^2}{16} \frac{\sin(\sqrt{3}-1)(\theta + \lambda)}{(1-2\sqrt{3})} + \frac{\sin(\sqrt{3}+1)(\theta + \lambda)}{(1+2\sqrt{3})} \\
& + \frac{4}{\sqrt{3}} C_{11} \cos(2\theta + \phi_{11}) + \frac{4}{\sqrt{3}} C_{12} \cos(\lambda + \phi_{12}) + \frac{4}{\sqrt{3}} C_{15} \cos(\sqrt{3}-1)\theta + \phi_{15}) \\
& + \frac{4}{\sqrt{3}} C_{18} \cos((\sqrt{3}+1)\theta + \phi_{18}) + A(3e + \lambda_c) \cos \theta \cos \sqrt{3}(\theta + \lambda) \\
& + B(3e + \lambda_c) \cos \theta \sin \sqrt{3}(\theta + \lambda) + \frac{4}{\sqrt{3}} C_1 (3e + \lambda_c) \cos \theta \cos(\theta + \phi_1) \\
& + \frac{4}{\sqrt{3}} C_8 (3e + \lambda_c) \cos \theta \cos(\sqrt{3}\theta + \phi_8) + A \lambda_s \sin \theta \cos \sqrt{3}(\theta + \lambda) \\
& + B \lambda_s \sin \theta \sin \sqrt{3}(\theta + \lambda) + \frac{4}{\sqrt{3}} C_1 \lambda_s \sin \theta \cos(\theta + \phi_1) \\
& + \frac{4}{\sqrt{3}} C_8 \lambda_s \sin \theta \cos(\sqrt{3}\theta + \phi_8)] \tag{2.64}
\end{aligned}$$

The variational equations for the total angular momentum  $L$ , the orbital eccentricity,  $e$ , the semimajor axis,  $a$ , and the

argument of pericenter,  $\omega$ , may be written in terms of the perturbing radial and tangential accelerations as (Ref 7),

$$\frac{dL}{d\theta} = \frac{R^3}{L} a_{\theta} \quad (2.65)$$

$$\frac{de}{d\theta} = \frac{R^2 p}{L^2} [\sin\theta] a_r + [\cos\theta + \frac{R}{p}(e + \cos\theta)] a_{\theta} \quad (2.66)$$

$$\frac{da}{d\theta} = \frac{2R^2 a^2}{L^2} [e(\sin\theta) a_r - \frac{p}{R} a_{\theta}] \quad (2.67)$$

$$\frac{d\omega}{d\theta} = \frac{-R^2}{eL^2} [p(\cos\theta) a_{\theta} - (p+R)(\sin\theta) a_r] \quad (2.68)$$

By substituting equations (2.63) and (2.64) into equations (2.65), (2.66), (2.67) and (2.68), and linearizing to second order in  $l/R$  as well as in  $e$ ,  $\lambda_c$ ,  $\lambda_s$ ,  $A$  and  $B$ , one obtains a set of nonperiodic variational equations which can not be averaged directly over one orbit. Each term in these equations, however, may be written in terms of first powers of sine and cosine, and thus may be averaged separately according to its particular frequency. Using this technique of averaging, results in the following equations describing

the average changes in the orbital elements due to tether orbital resonance.

$$\frac{dL}{d\theta}_{\text{avg}} = 0 \quad (2.69)$$

$$\frac{de}{d\theta}_{\text{avg}} = -6 \frac{m_{12}}{m} \left(\frac{\bar{l}}{a}\right)^2 \lambda_s \quad (2.70)$$

$$\frac{da}{d\theta}_{\text{avg}} = -12 \frac{m_{12}}{m} \left(\frac{\bar{l}}{a}\right)^2 e \lambda_s \quad (2.71)$$

$$\frac{d\omega}{d\theta}_{\text{avg}} = 6 \frac{m_{12}}{m} \left(\frac{\bar{l}}{a}\right)^2 \left(1 + \frac{\lambda_c}{e}\right) \quad (2.72)$$

Equation (2.69) states that the total angular momentum of the center of mass must be conserved on average. This is consistent with the fact that the overall angular momentum is strictly constant due to the central nature of the external forces (Appendix A), while the angular momentum with respect to the center of mass remains bounded. Of course, the angular momentum of the center of mass does fluctuate in the course of each orbit, in response to the corresponding fluctuations of the libration angle.

The average rate of change in orbital eccentricity,

described in equation (2.70), agrees with Martinez's result given in equation (8). This change is directly proportional to  $\lambda_s$ , the constant of the sine term of the tether length equation (2.23). Therefore, only the variation of the tether length in spacial quadrature with the radius vector magnitude contributes to the change in eccentricity. If  $\lambda_s$  is positive (in the direction of the true anomaly), a decrease in orbital eccentricity will result and vice versa. Thus, an orbit can be gradually circularized by "paying out" tether during perigee passage, i.e., so as to have maximum deployed length  $90^\circ$  past the perigee. Notice the absence of quadratic terms in equation (2.70) and (2.72). These results are accurate to second order, though, and the error involved is cubic in  $\alpha$ ,  $e$ ,  $\lambda_s$ , and  $\lambda_c$ .

Since the average angular momentum is constant, a decrease in orbital eccentricity will correspondingly yield a decrease in the semimajor axis. Equation (2.71) describes how the semimajor axis varies to second order with both the eccentricity and the constant  $\lambda_s$ . Here we note the absence of first order terms in  $e$ ,  $\alpha$ ,  $\lambda_s$  and  $\lambda_c$ . Indeed, small eccentricity changes in a near-circular will not affect the orbit's energy or semimajor axis. This follows from the Keplerian relationship given in equation (2.75), which is

satisfied to second order in  $e$  by equation (2.69), (2.70), and (2.71).

The cosine term of the tether length equation (which produces a maximum tether length at perigee and a minimum tether length at apogee) yields a positive rotation in the argument of perihelion as described in equation (2.72). This rotation is also inversely proportional to the eccentricity. The constant term in equation (2.72), describes a constant rate of change of the argument of perihelion due to the fact that the tether system is a very elongated mass whose forced libration due to orbital eccentricity alone (even with no tether length changes) is in resonance with the orbital motion.

By integrating equations (2.69), (2.70), (2.71) and (2.72), it is now possible to find closed form solutions for these parameters in terms of  $\theta$ .

Equation (2.70) may be written as follows:

$$\frac{d_e}{d\theta}_{avg} = -C \left(\frac{1}{2}\right) \quad (2.73)$$

where,

$$C = 6 \frac{m_{12}}{m} \left(\frac{\bar{l}}{p}\right)^2 p^2 \lambda_s \quad (2.74)$$

C is constant on average, since angular momentum and therefore the orbital parameter, p, are constant on average. Now, consider the relationship between the total angular momentum, the semimajor axis, and the orbital eccentricity.

$$L^2 = \mu a(1-e^2) \quad (2.75)$$

Solving for "a" in terms of "e", substituting into equation (2.73), and separating variables yields an integrable equation for the eccentricity. Using the initial conditions at  $\theta = 0.0$ ,  $e = e_0$ , one obtains the following closed form solution for the eccentricity:

$$e = \frac{\sqrt{2}}{2} \tanh \left[ -\frac{N}{N^*} + \tanh^{-1}(\sqrt{2}e_0) \right] \quad (2.76)$$

where,

$$N = \frac{\theta}{2\pi} = \# \text{ of orbits completed} \quad (2.77)$$

$$\frac{1}{N^*} = 12\sqrt{2}\pi \frac{m_{12}}{m} \left(\frac{\bar{x}}{p}\right)^2 \lambda_s \quad (2.78)$$

This equation describes the eccentricity as a monotonically decreasing function of  $N/N^*$ , starting at  $e_0$  and reaching a minimum limit at  $e = -.7071$ . The eccentricity must be positive, however, giving a real minimum limit of  $e=0.0$ . A

graph of equation (2.76) for a positive  $\lambda_s$  is shown in Figure 5. Note that  $N^*$  is negative if  $\lambda_s$  is (thus yielding an increase of  $e$  with  $\theta$ ). Of course the quadratic approximation and other aspects of the theory, such as the boundedness of  $\alpha$  fail for large values of  $e$ .

By substituting equation (2.75) into equation (2.73) and integrating, one obtains a similar expression for the semimajor axis divided by the parameter.

$$\frac{a}{p} = 1 + 1/2 \tanh^2 \left[ -\frac{N}{N^*} + \tanh^{-1}(\sqrt{2} e_0) \right] \quad (2.79)$$

This ratio is a monotonically decreasing function of  $N/N^*$ , originating at  $a/p=1+e_0^2$  and reaching a minimum at  $a/p=1.0$  (since  $e$  must remain positive). A plot of this equation for a positive  $\lambda_s$  is given in Figure 6.

Finally, one can obtain a closed form solution for the argument of pericenter,  $\omega$ , by first writing equation (2.72) as

$$\frac{d\omega}{d\theta}_{\text{avg}} = \frac{D}{a} \left( 1 + \frac{\lambda_c}{e} \right) \quad (2.80)$$

where,

$$D = 6 \frac{m_{12}}{m} \left( \frac{\bar{g}}{p} \right)^2 p^2 \quad (2.81)$$



Dividing equation (2.80) by equation (2.73) and integrating subject to the initial condition at  $\omega=0.0$ ,  $e=e_0$ , one obtains the following result.

$$\omega = -\frac{1}{\lambda_s} \left[ \frac{\sqrt{2}}{2} \tanh \left( -\frac{N}{N^*} + \tanh^{-1} [\sqrt{2} e_0] \right) - e_0 \right. \\ \left. - \lambda_c \ln \left( \frac{\sqrt{2}}{2e_0} \tanh \left[ -\frac{N}{N^*} + \tanh^{-1} (\sqrt{2} e_0) \right] \right) \right] \quad (2.82)$$

A plot of this equation for a positive  $\lambda_s$  and  $\lambda_c=0.0$ , is given in Figure 7.

### III. Theoretical Analysis versus Numerical Analysis

In this section, the theoretical variations of the orbital parameters derived in Section II, will be compared to purely numerical results obtained by integrating the equations of motion of the center of mass of the tether system (equations (2.18), (2.19) and (2.20)).

As mentioned in Section II, it is the sine variation of the tether length that produces a change in the orbital eccentricity. A positive  $\lambda_s$  will result in a decreasing orbital eccentricity, and a negative  $\lambda_s$  will result in an increasing orbital eccentricity. A cosine variation of the tether length will simply effect the rotation of the argument of perihelion. A positive  $\lambda_c$  will result in a positive rotation of the argument of perihelion. A negative  $\lambda_c$  will result in either a positive or a negative rotation in the argument of perihelion depending on the ratio  $\lambda_c/e$  (positive, if  $|\lambda_c/e|$  is less than or equal to 1, negative otherwise).

Three potential tether missions will be considered:

- 1) A decrease in orbital eccentricity using a sine variation of the tether length ( $\lambda_s$  positive,  $\lambda_c=0.0$ , a maximum tether length  $90^\circ$  past perigee and a minimum tether length  $90^\circ$  before perigee)
- 2) An increase in orbital eccentricity using a sine variation of the tether length ( $\lambda_s$  negative,  $\lambda_c=0.0$ , a minimum tether length  $90^\circ$  past perigee and a maximum tether length  $90^\circ$  before perigee)

- 3) A constant orbital eccentricity using a cosine variation of the tether length ( $\lambda_c$  positive,  $\lambda_s = 0.0$ , a maximum tether length at perigee and a minimum tether length at apogee)

Tether velocity, tether tension, and the power required for the tether reeling operation will be considered for the first case. The instantaneous tether tension for a length varying tether is derived in Appendix B and is given by

$$\begin{aligned}
 T = & -\frac{\mu}{R^3} m_{12} \ell [-2 + 3\sin^2 \alpha] \\
 & - \frac{3\mu}{R^4} \ell^2 \cos \alpha [1 - \frac{5}{2}\sin^2 \alpha] \frac{m_{12}}{m} [m_1 - m_2] \\
 & - \ddot{\ell} m_{12} + \ell m_{12} (\ddot{\alpha} + \dot{\theta})^2
 \end{aligned} \tag{3.1}$$

The instantaneous power is simply the product of the tether tension and velocity.

$$P = T \left( \frac{d\ell}{dt} \right) \tag{3.2}$$

$$\frac{d\ell}{dt} = \bar{\ell} (\alpha_s \cos \theta - \alpha_c \sin \theta) \frac{d\theta}{dt} \tag{3.3}$$

For all cases considered, the following initial conditions were used:

$$m_1 = 100,000 \text{ kg}$$

$$m_2 = 10,000 \text{ kg}$$

$$l = 100 \text{ km}$$

$$R_p = 6770 \text{ km}$$

$$\mu = 398778 \text{ km}^3/\text{sec}^2$$

$$\theta = 0.0$$

$$A = 0.0$$

$$B = 0.0$$

A copy of the program used to calculate the following results is given in Appendix C. Numerical integration of the equations of motion was executed using fourth order Runge Kutta, with a  $10^\circ$  step size. Double precision accuracy was used to minimize roundoff errors.

### 3.1 Decreasing Orbital Eccentricity Using a Sine Variation of the Tether Length

As a first example, consider  $\lambda_s = 0.2$ ,  $\lambda_c = 0.0$ , and an initial eccentricity  $e = 0.1$ . For  $\lambda_s = 0.2$ , a sinusoidal length variation between 80 and 120 kilometers results, with a maximum tether length  $90^\circ$  past perigee and a minimum tether length  $90^\circ$  prior to perigee. A graph of the tether length versus the true anomaly is given in Figures 8 and 9.

Figures 10 and 11, show the changes in the Coriolis induced in-plane libration angle as a function of the number

of orbits completed. The libration angle is a nonperiodic, bounded function with a maximum value of  $24^\circ$ .

The analytical and numerical eccentricity, semimajor axis, and argument of perihelion, are plotted versus the number of orbits completed in Figures 12, 13, and 14. As seen in Figure 12, the orbital eccentricity can be decreased from 0.1 to 0.0773 in 200 orbits or approximately 15 days. The theoretical eccentricity falls within 0.76 % of the numerical eccentricity, and the theoretical semimajor axis falls within 0.02 % of the numerical semimajor axis. Thus, the analytical expressions derived in Section II for both the eccentricity and the semimajor axis are very good approximations describing the variations of these elements. In Figure 14, the numerical argument of perihelion increases by  $9.7^\circ$ , while the theoretical argument of perihelion predicts only a  $6.5^\circ$  change after 200 orbits (within 33 % of the numerical value). For better accuracy, one would have to consider third and higher order terms not kept in the theoretical analysis.

Next, consider the tether velocity, tension and power requirements given in Figures 15 through 20. In Figures 15 and 16, the tether velocity is seen as a near sinusoidal variation, with a 24 m/s maximum speed. A positive velocity signifies an increasing tether length, while a negative velocity signifies a decreasing tether length. Note, the

tether velocity has a larger magnitude for an increasing tether length than a decreasing tether length. This may be explained by the fact that the center of mass angular velocity,  $d\theta/dt$ , in equation (3.2) is maximum at perigee and a negative libration angle (or a rotation of the tether about the system c.m., opposite to the rotation of the tether system in its orbit) and minimum at apogee and a positive libration angle. The above is consistent with equation (2.20), describing the conservation of total angular momentum.

The instantaneous tether tension, described by equation (3.1), is plotted as a function of the number of orbits completed in Figures 17 and 18. The maximum and minimum tensions which occur during the mission are approximately 4000 and 1500 Newtons respectively. Note, the minimum tether tension is sufficiently high, far from the danger of a zero tension tether. The average tether tension is approximately 2750 N.

In Figures 19 and 20, the power required for the tether reeling operation is given as a function of the number of orbits completed. A positive power corresponds to a power consumption (tether length decreasing by reeling process), and a negative power corresponds to a power dissipation or storage (tether length increasing due to external forces). The power consumed exceeds the power dissipated or stored by a factor of

2.6, which is a desirable result since it is best to have a minimum amount of power to be dissipated.

The peak power required is approximately 90 kilowatts and occurs when the product of the tether velocity and tension is maximum, according to equation (3.3). The maximum power to be dissipated and the average power are approximately 30 and 15 kilowatts respectively. A means of measuring the relative inefficiency of designing a 90 kilowatt power supply for operating the tether system is to consider the average to peak power ratio which is approximately 0.17, compared to an ideal ratio of unity. Of course the maximum power required can be significantly decreased by using a shorter tether, having the effect that it will take a longer operation time to obtain the same variations in the orbital parameters.

Finally, it is important to consider the range of values of the initial eccentricity, and  $\lambda_s$  for which the tether libration angle remains bounded. In Figure 21, the maximum libration angle encountered during a mission is plotted versus the initial eccentricity (this assumes  $\lambda_s = 0.2$ ,  $\lambda_c = 0.0$ ). For values of the original eccentricity greater than 0.16, the tether angle is unbounded, and the tether system starts to spin. In Figure 22, the maximum libration angle encountered during a mission is plotted versus the constant  $\lambda_s$  (this assumes an initial eccentricity  $e = 0.1$ , and  $\lambda_c = 0.0$ ). For

values of  $\lambda_s$  greater than 0.27, the tether angle is again unbounded, and the tether system starts to spin. A graph demonstrating the maximum initial eccentricity and  $\lambda_s$  combinations possible before an instability in the tether libration angle occurs is given in Figure 23. The area below the curve represents a tether system with a bounded libration angle, while the area above the curve represents a spinning tether system.

### 3.2 Increasing Orbital Eccentricity Using a Sine Variation of the Tether Length

This section will verify that the tether scheme of section 3.1 is reversible, i.e. that the eccentricity of the orbit may be increased using tether orbital resonance. For this mission, let  $\lambda_s = -0.2$ ,  $\lambda_c = 0.0$  and the initial eccentricity be  $e = 0.0773$  (this was the final eccentricity obtained after 200 orbits in section 3.1). With  $\lambda_s = -0.2$ , the tether length will reach a minimum value  $90^\circ$  after perigee, and a maximum value  $90^\circ$  prior to perigee. The variations in the tether length and libration angle are given in Figures 24 and 25.

As seen in Figures 26 and 27, after 200 orbits, the eccentricity and semimajor axis have increased to the



eccentricity and semimajor axis values used as initial conditions in section 3.1 ( $e = 0.1$ , and  $a = 7521$  km). Thus, the eccentricity and semimajor axis are directly reversible. Again, the analytical eccentricity and semimajor axis are within 0.16 % and 0.004 % of their numerical values.

In Figure 28, both the theoretical and numerical analysis show a positive rotation in the argument of perihelion. After 200 orbits, the numerical analysis yields a  $5.2^\circ$  rotation of the argument of perihelion, while the theoretical analysis predicts a  $6.3^\circ$  rotation of the argument of perihelion (within 21% of the numerical value). Again, the theoretical model must consider third and higher order terms in equation (2.82) to predict the variation in the argument of perihelion more accurately.

### 3.3 Constant Orbital Eccentricity Using a Cosine Variation of the Tether Length

As a final example, let  $\lambda_s = 0.0$ ,  $\lambda_c = 0.2$  and the initial eccentricity be equal to  $e=0.1$ . Under these conditions, the tether length will reach a maximum value at perigee and a minimum value at apogee. The variations in tether length and libration angle for this mission may be seen in Figures 29 and 30.

According to equations (2.70) and (2.71), setting  $\lambda_s=0.0$  (i.e. no sine term in the tether length equation) will result in a zero net change in the orbital eccentricity and semimajor axis. The numerical results verify this in Figures 31 and 32. In fact, the final eccentricity and semimajor axis are within 0.04 % and 0.12 % of their original values (therefore, any deviation in the numerical results may be regarded as noise).

Looking at equation (2.72) a positive  $\lambda_c$  value should result in an additional positive rotation of the argument of perihelion compared to the rotation if  $\lambda_c=0.0$  (as in Section 3.1). This theoretical variation in the argument of perihelion is shown in Figure 33, and reaches  $18.93^\circ$  after 200 orbits (compared to  $6.5^\circ$  for  $\lambda_c=0.0$ ). The numerical value of the argument of perihelion reaches  $20.02^\circ$  after 200 orbits (compared to  $9.7^\circ$  for  $\lambda_c=0.0$ ). For this example, the theory is able to predict the argument of perihelion to within 6 % of its actual value.

#### IV. Conclusion

Linearized approximations (to second order in  $\ell/R$ ,  $e$ ,  $\lambda_s$ , and  $\lambda_c$ ) for the variations of the orbital elements due to tether orbital resonance were derived in Section II. In Section III these approximations were compared to the variations obtained by integrating the equations of motion. The theoretical variations of both the orbital eccentricity and semimajor axis were found to be very close to the numerical results (within 1 % after 200 orbits or 15 days). Although the theoretical estimate for the variation in the argument of perihelion was significantly less accurate than for the eccentricity and semimajor axis, it was still within 33 % of the numerical value in the worst case and 5.4 % of the numerical value in the best case examined.

The numerical analysis was extended to identify the range of values of the eccentricity and tether length parameter  $\lambda_s$  for which the libration angle remains bounded for a sinusoidal variation in tether length. The instantaneous tether tension equation derived in Appendix B allowed for the calculation of both the tether tension and the power required for operation of the tether system.

The derivation and verification of the linearized, second order variations in the orbital elements due to tether orbital resonance, increases the confidence with which potential

missions may be studied. It has been shown that significant changes in eccentricity may be obtained using a sinusoidal, length varying tether system within a reasonable period of time and varying power demands. Due to the relatively large power requirement necessary to make the resonance scheme competitive with other orbital maneuver techniques, a space station application seems the most likely candidate (since a large power source would be present for other station requirements). A space platform could change orbits at virtually no expense simply by deploying a length varying tether in times of off-peak power requirements. Of course, not all possible orbital changes could be conducted using a tether system, since the total angular momentum must remain constant. Several practical applications of the resonance technique are possible, however, especially in cooperation with other potential tether applications. For example, the elliptic orbit that results after a station deploys a satellite or deboosts the shuttle using a tether, could be recircularized using the same tether system by periodically varying the tether length. Several examples of this technique for various satellite masses and tether lengths were investigated in Reference 8. A cosine variation of the tether length, opens a new door in the potential use of a tether system for controlled rotation the argument of perihelion.

## REFERENCES

1. Tsiolkovsky, K. E., 1895, Grezy O. Zemie i nebe (i) Na Veste (Speculations between earth and sky, and on Vesta; science fiction works). Moscow, izd-vo AN SSSR, 1959, p. 35.
2. Beletskii, V. V., " The Motion of an Artificial Satellite in Relation to the Center of Masses ", in " Science ", 1968.
3. Beletskii, V. V., Givertz, M.E., Space Research, Vol VI, 1968, USSR.
4. Martinez-Sanchez, Manuel, " Modification of Orbital Energy by Control of Tether Length ", in Applications of Tethers in Space, Workshop Proceedings, Vol II, June 15-17, Williamsburg, VA.
5. Morse, P. M., and Feshbach, H., Methods of Theoretical Physics, New York, McGraw-Hill, Vol I, 1953.
6. Hildebrand, F. B., Advanced Calculus for Applications, Second Edition, Prentice-Hall Inc., New Jersey, 1976, pgs. 26-27.
7. Battin, R. H., Astronautical Guidance, New York, McGraw-Hill, 1964.
8. Martinez-Sanchez, M., Gavit, S. A., " Transportation Applications of Space Tethers ", Presented at the A.I.A.A./NASA Space Systems Technology Conference, Costa Mesa, CA, June 1984.

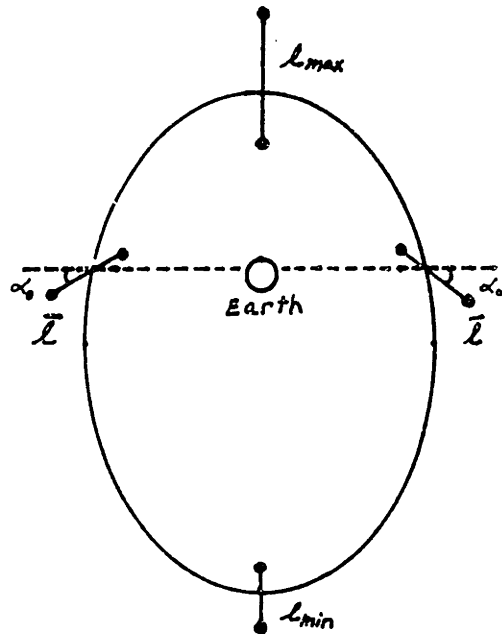


Figure 1. Sinusoidal Tether Libration Angle and Corresponding Length Variation Over One Orbit

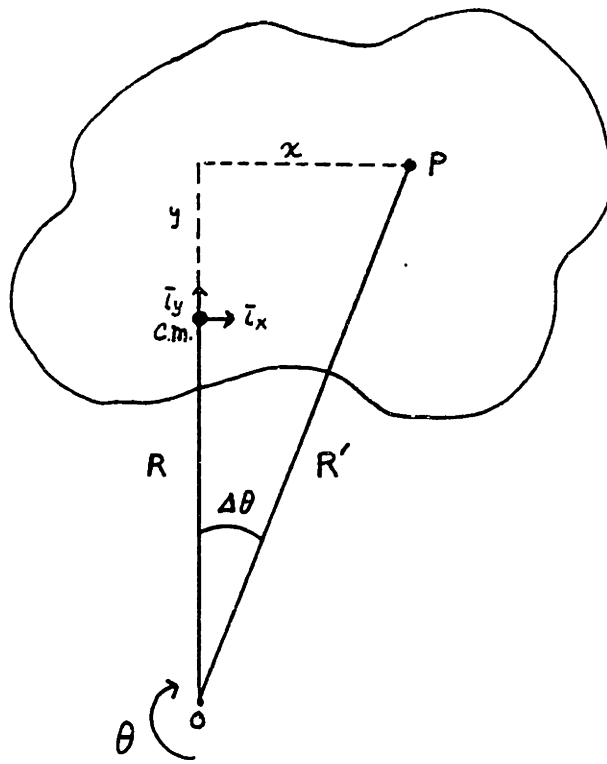


Figure 2. Geometry of an Orbiting Body

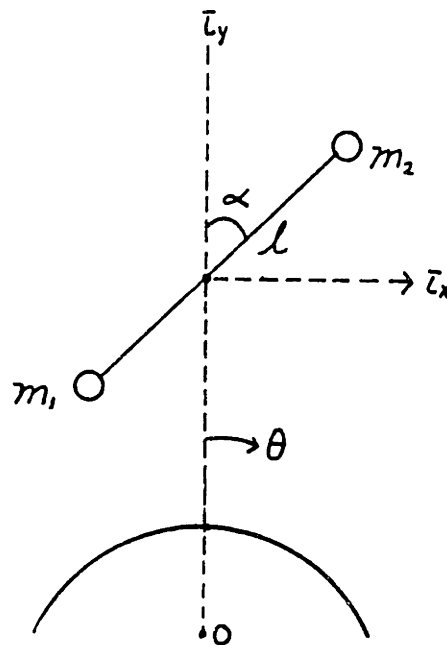


Figure 3. Geometry of an Orbiting Dumbbell

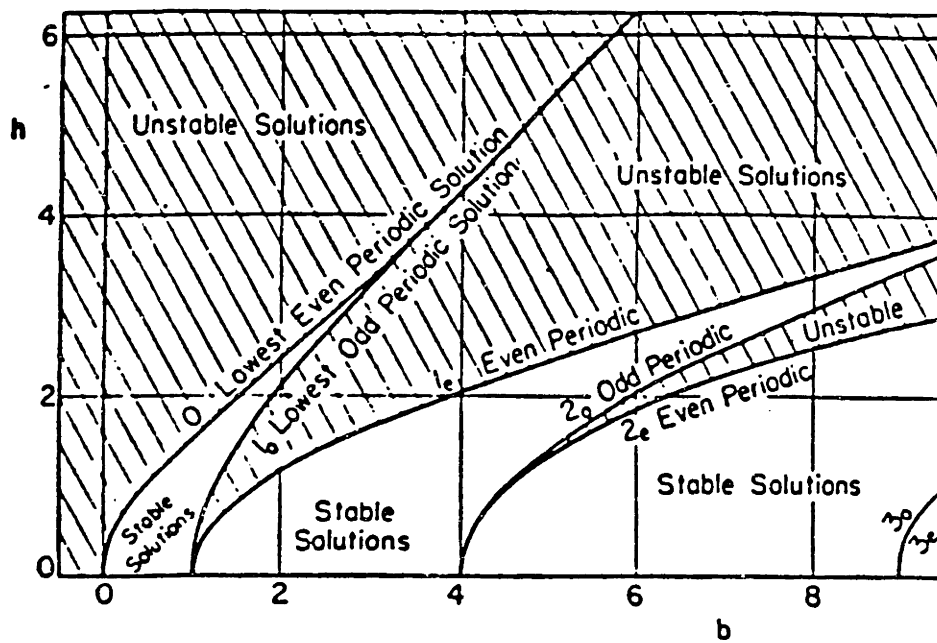


Figure 4. Mathieu's Stability Region



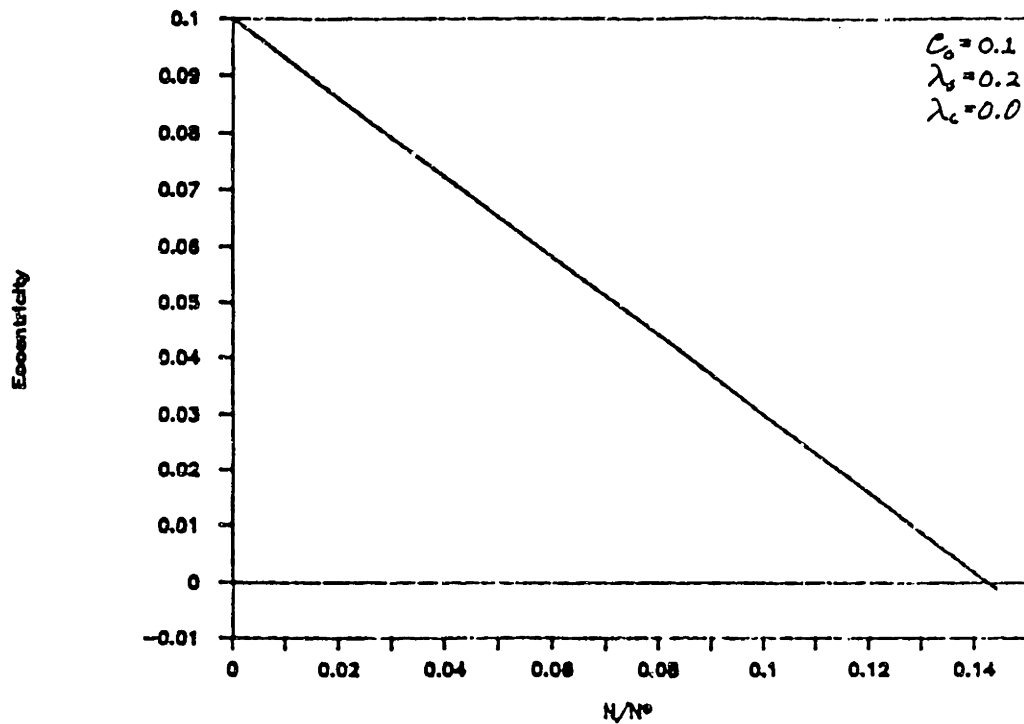


Figure 5. Eccentricity vs.  $N/N^*$

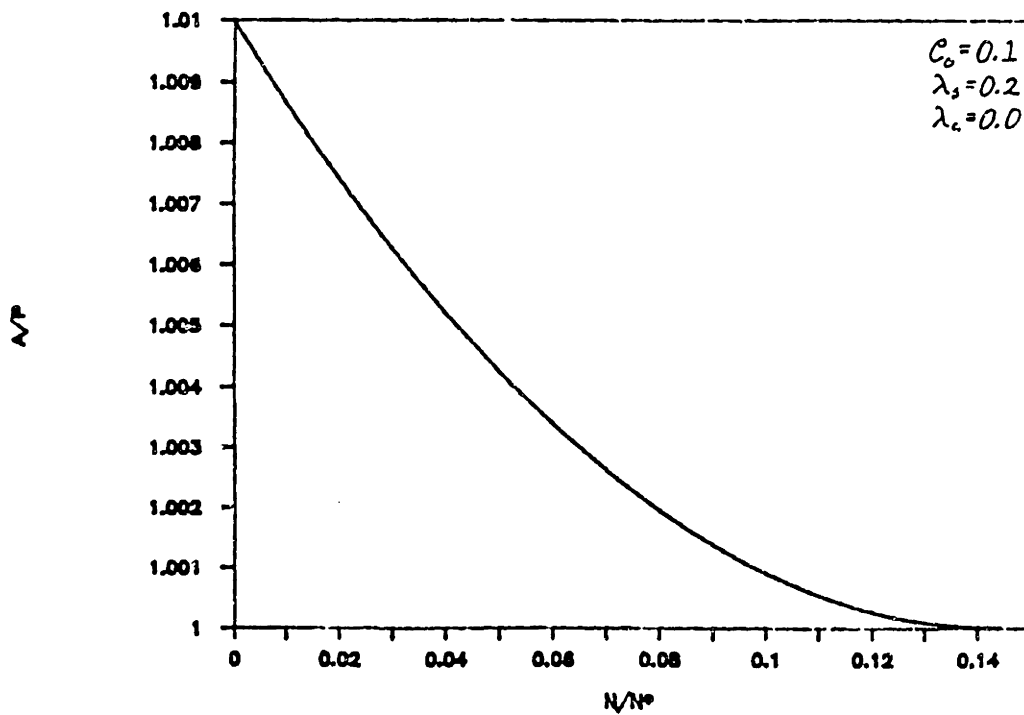


Figure 6.  $A/P$  vs.  $N/N^*$

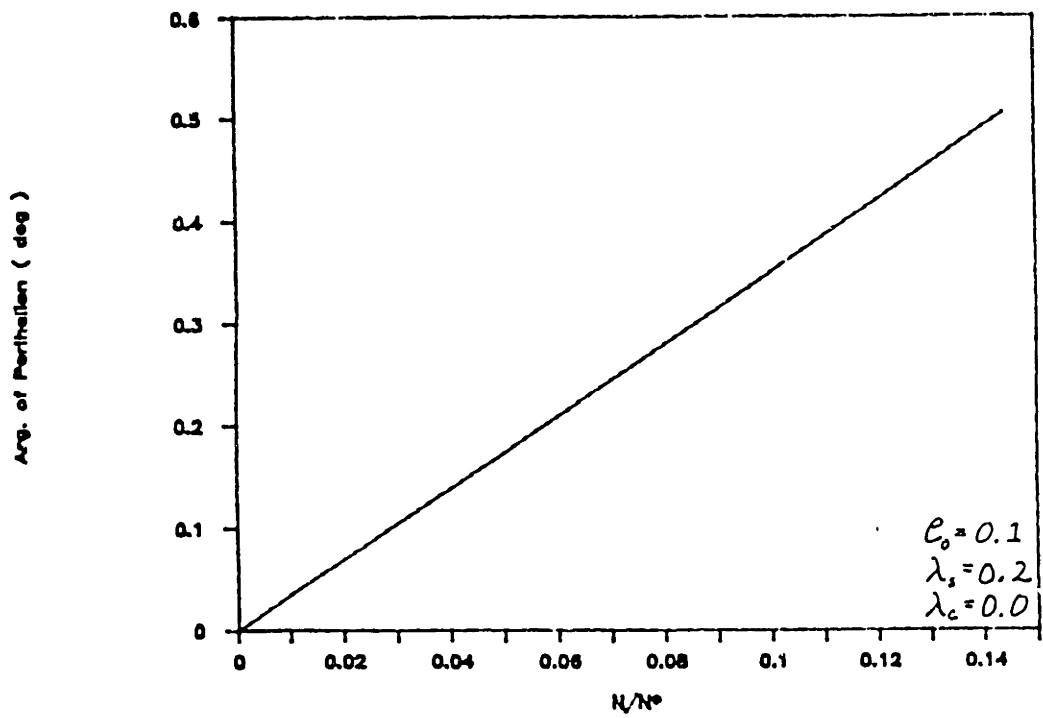


Figure 7. Arg. of Perihelion vs.  $N/N^*$

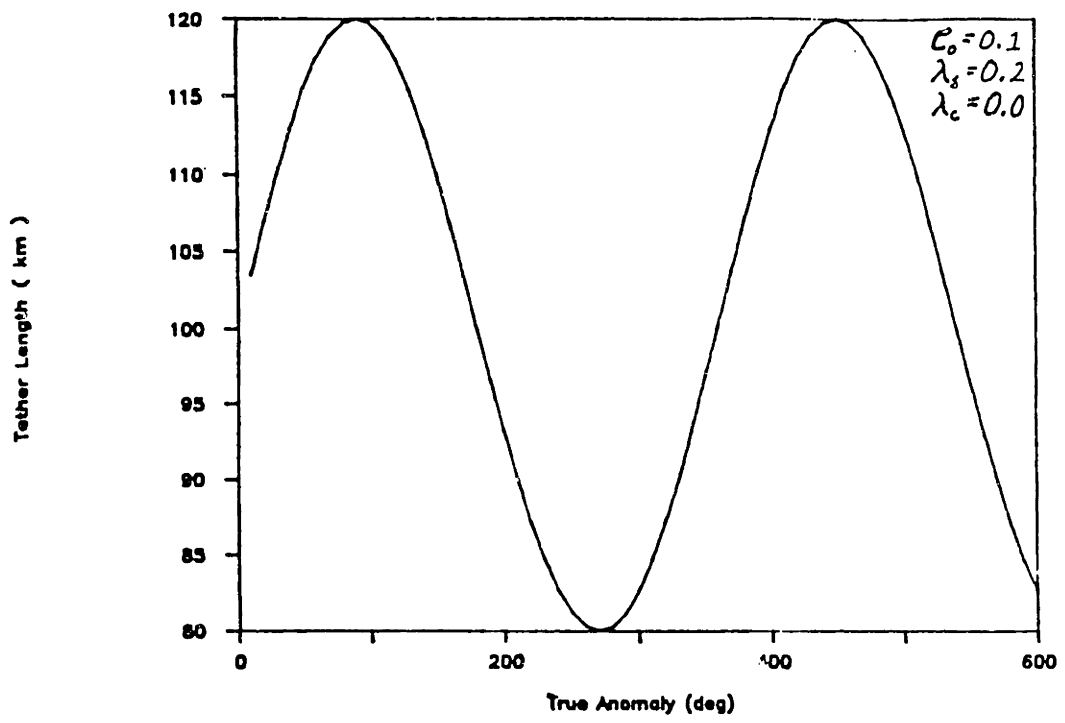


Figure 8. Tether Length vs. True Anomaly  
Over Two Orbits

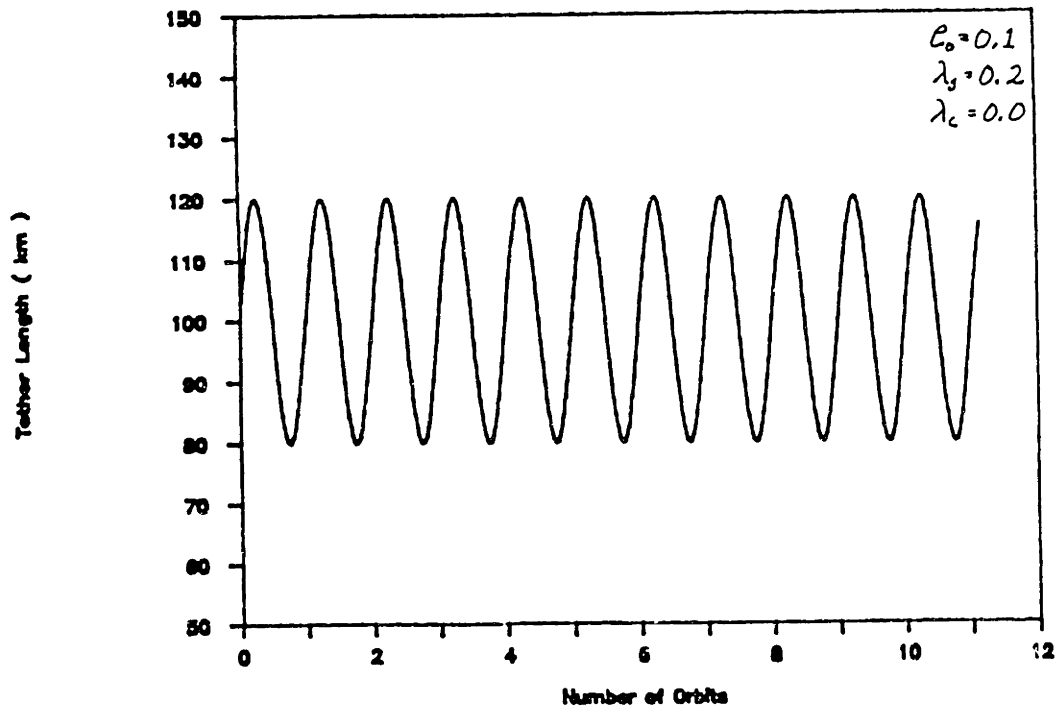


Figure 9. Tether Length vs. No. of Orbits  
Over Eleven Orbits

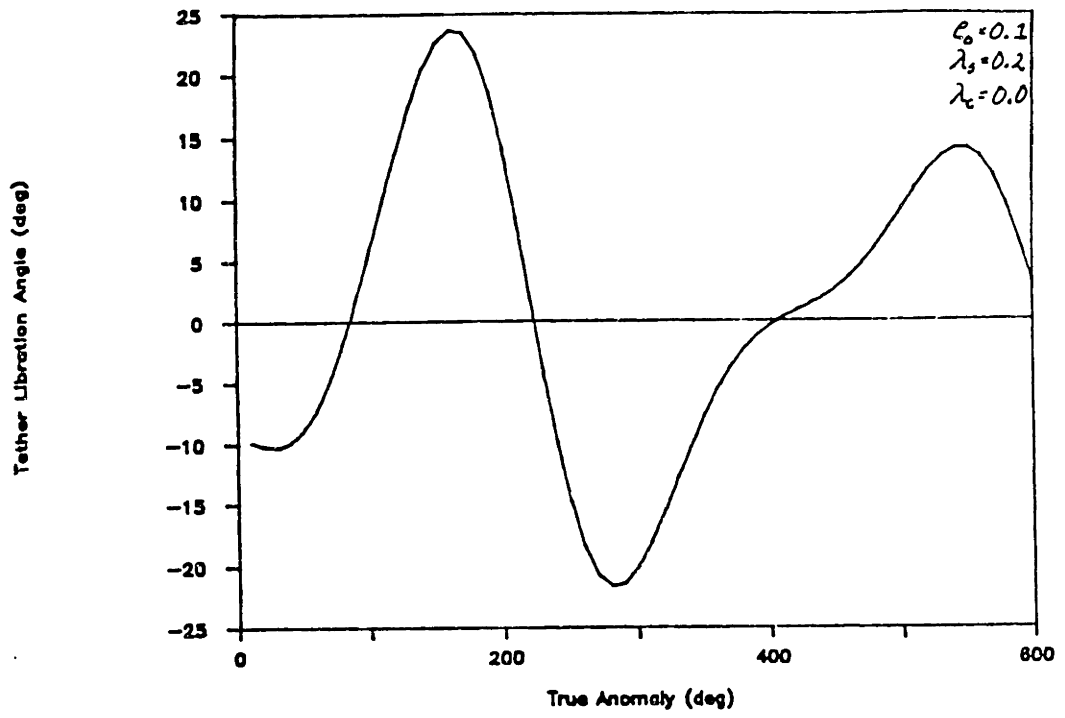


Figure 10. Tether Lib. Angle vs. True Anomaly  
Over Two Orbits

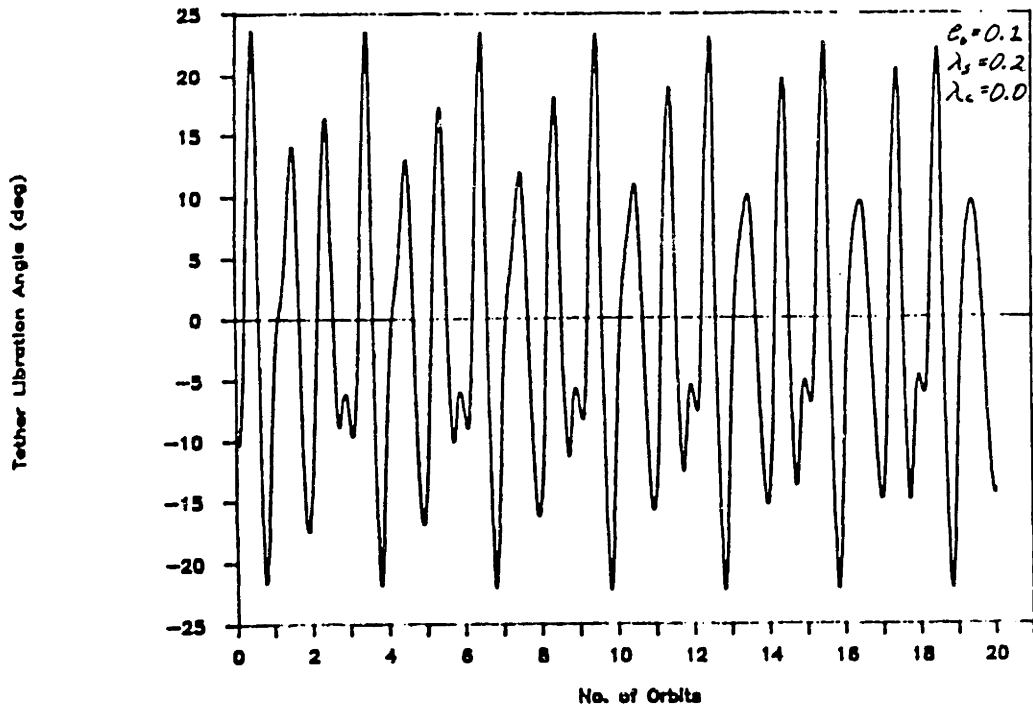


Figure 11. Tether Lib. Angle vs. No. of Orbits  
Over Twenty Orbits

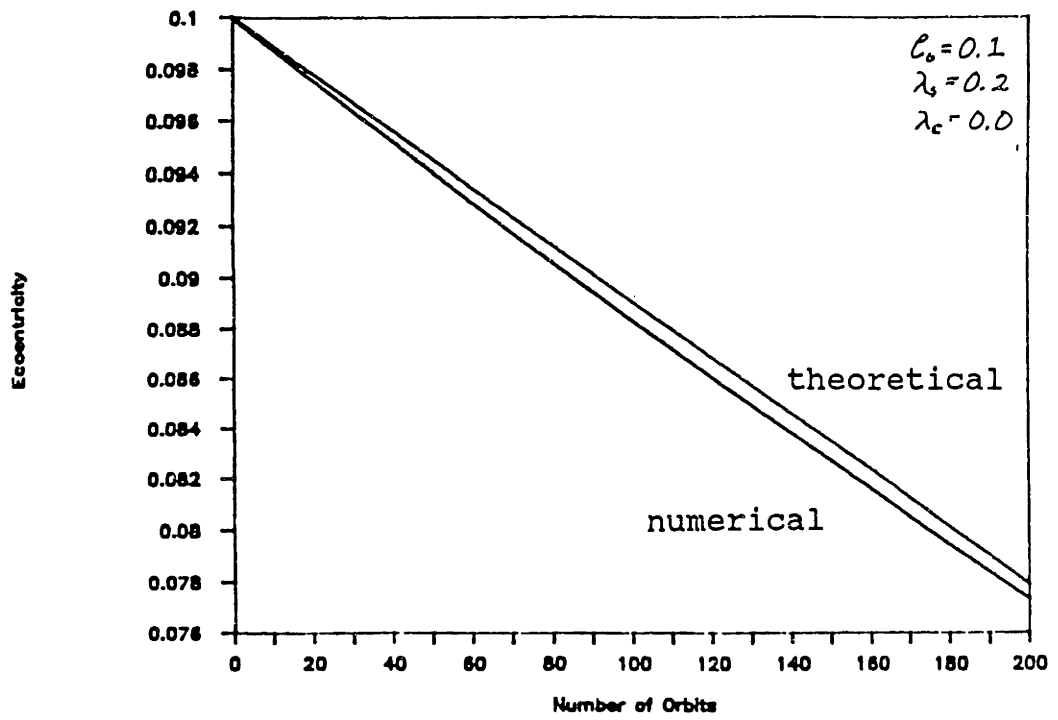


Figure 12. Eccentricities vs. No. of Orbits  
Analytical and Numerical

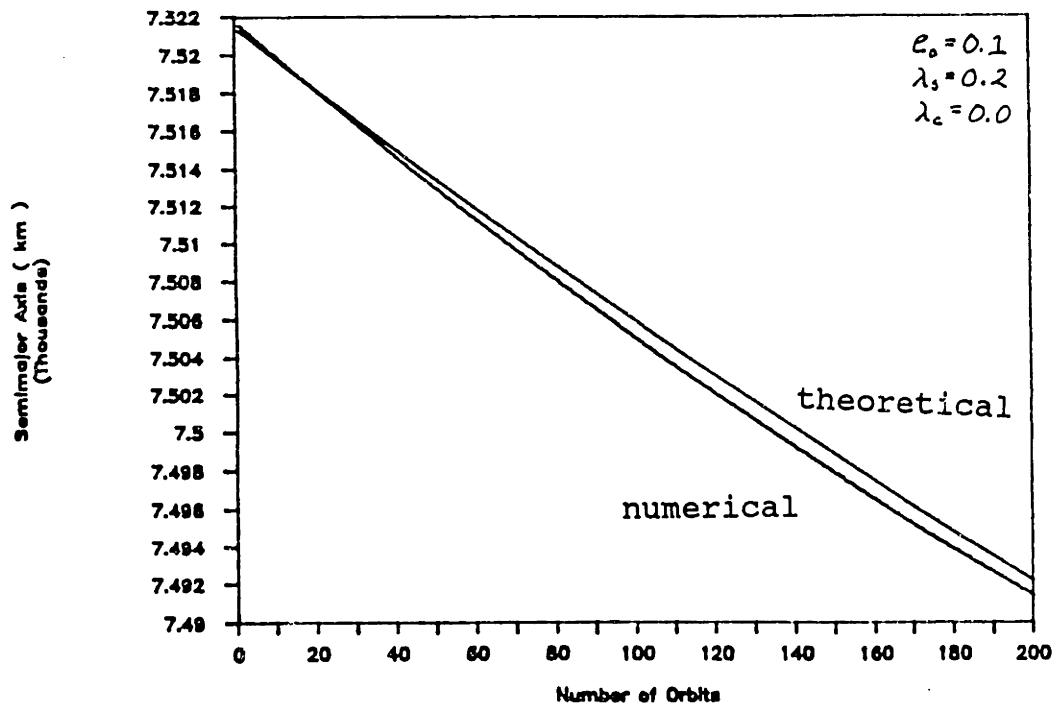


Figure 13. Semimajor Axis vs. No. of Orbits  
Analytical and Numerical

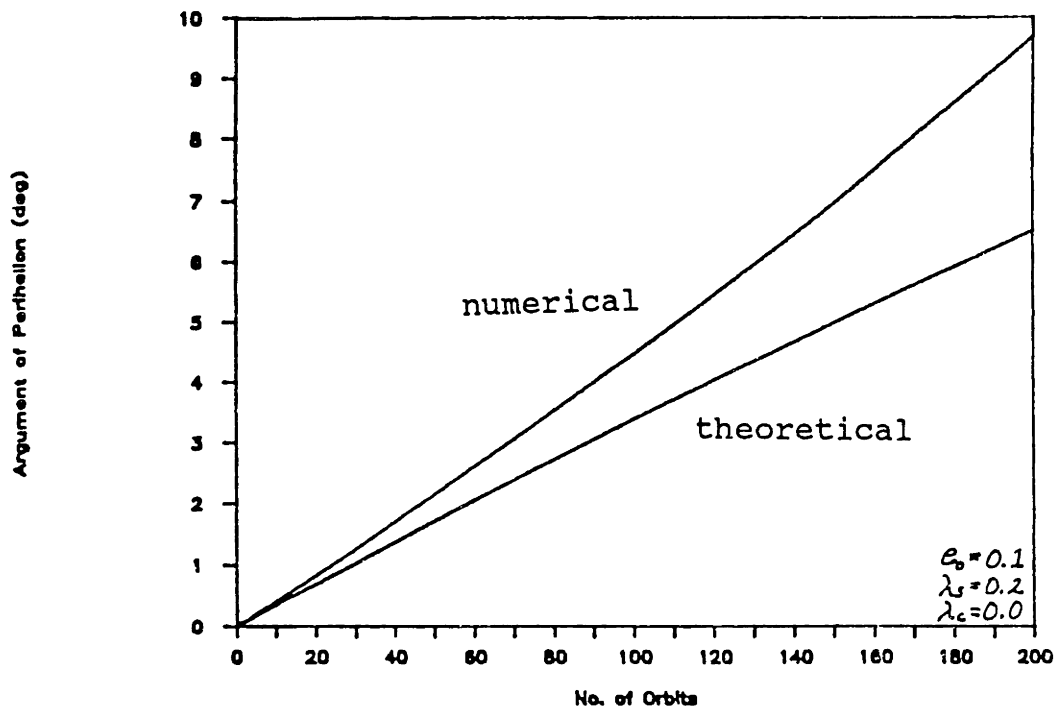


Figure 14. Arg. of Perihelion vs. No. of Orbits  
 Analytical vs. Numerical

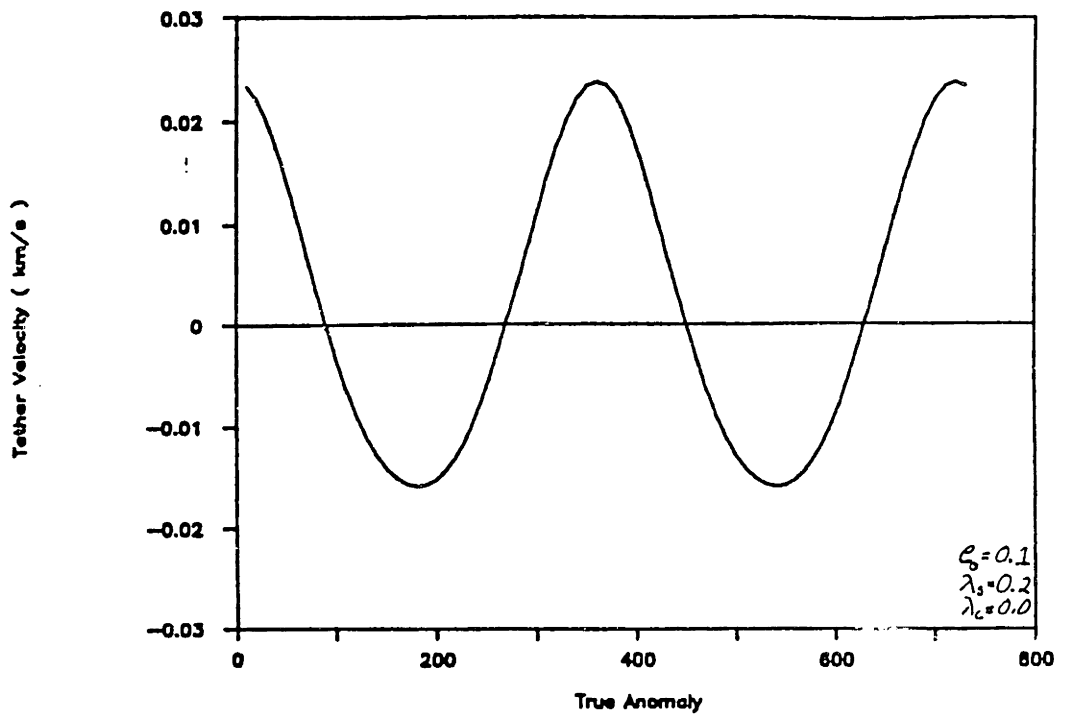


Figure 15. Tether Velocity vs. True Anomaly  
Over Two Orbits

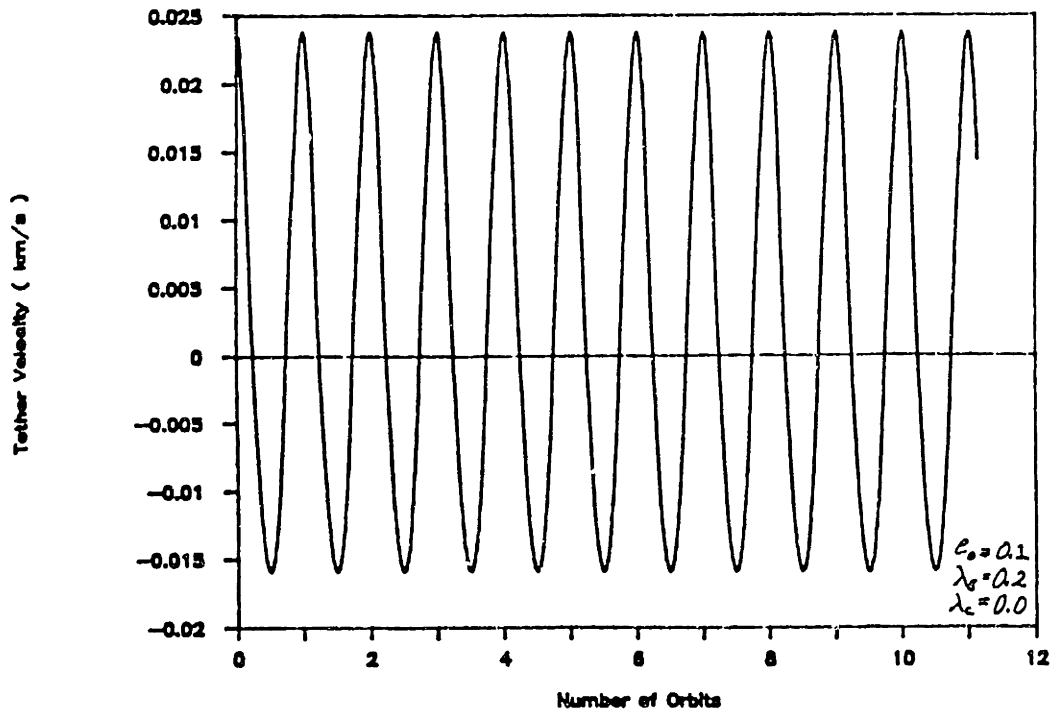


Figure 16. Tether Velocity vs. No. of Orbits  
Over Twelve Orbits

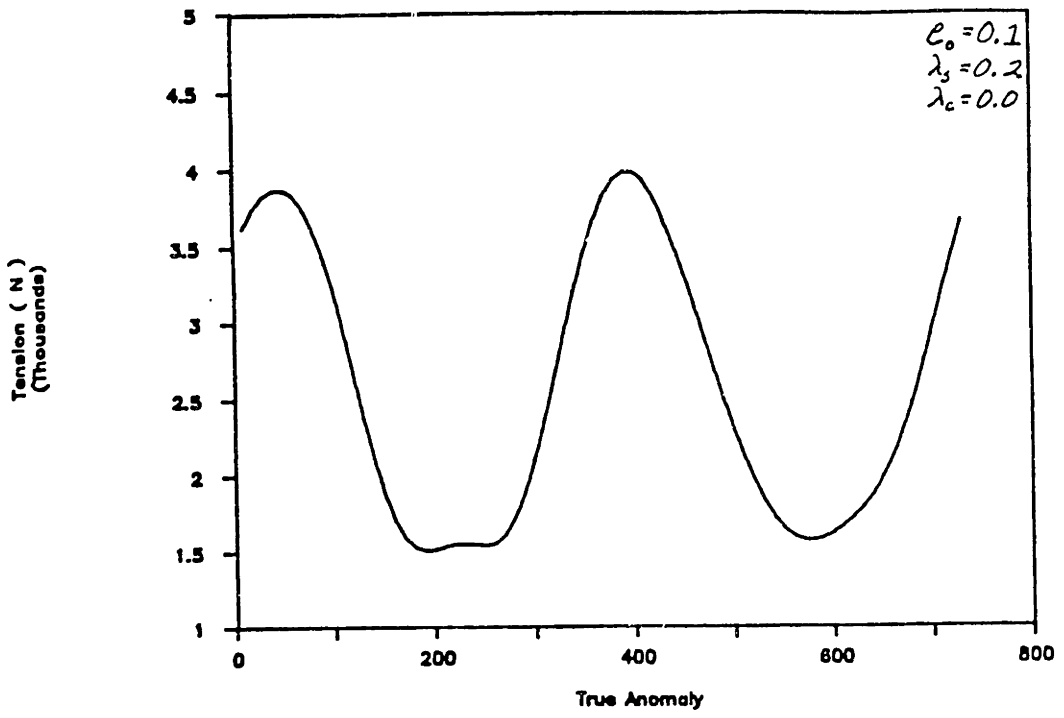


Figure 17. Tension vs. True Anomaly  
Over Two Orbits

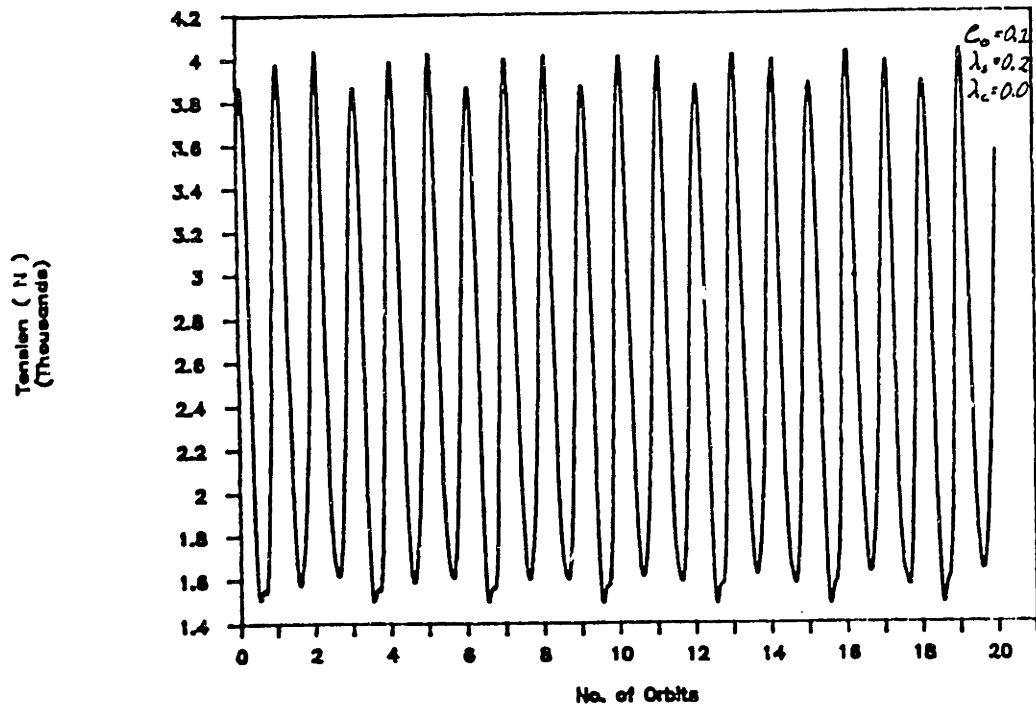


Figure 18. Tension vs. No. of Orbits  
Over Twenty Orbits



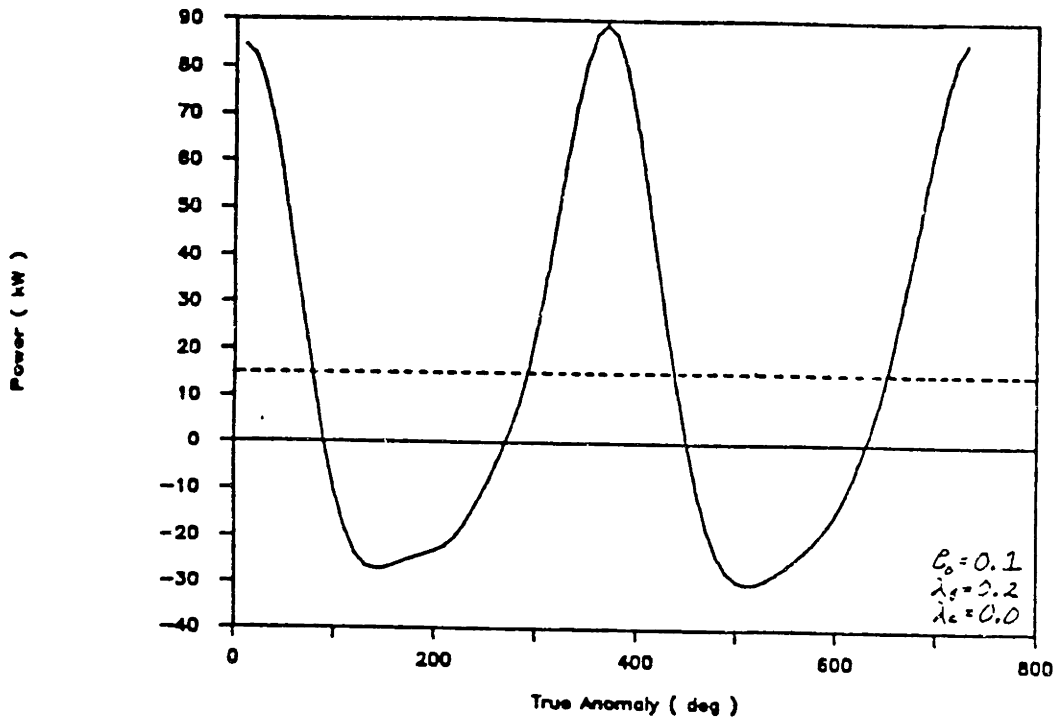


Figure 19. Power vs. True Anomaly  
Over Two Orbits

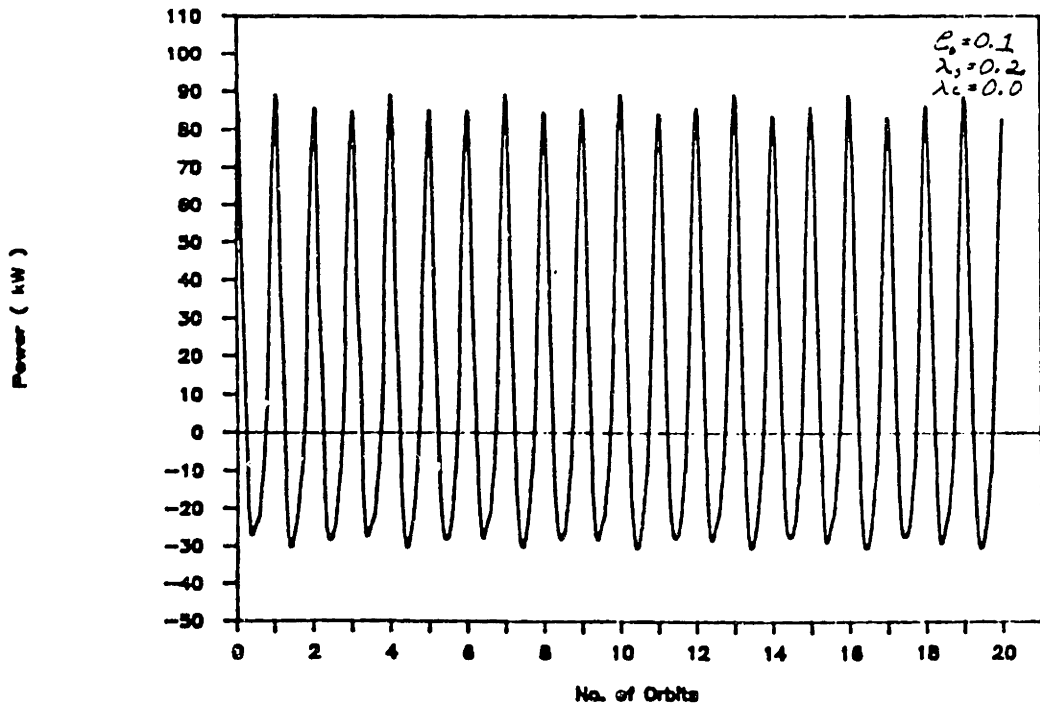


Figure 20. Power vs. No. of Orbits  
Over Twenty Orbits

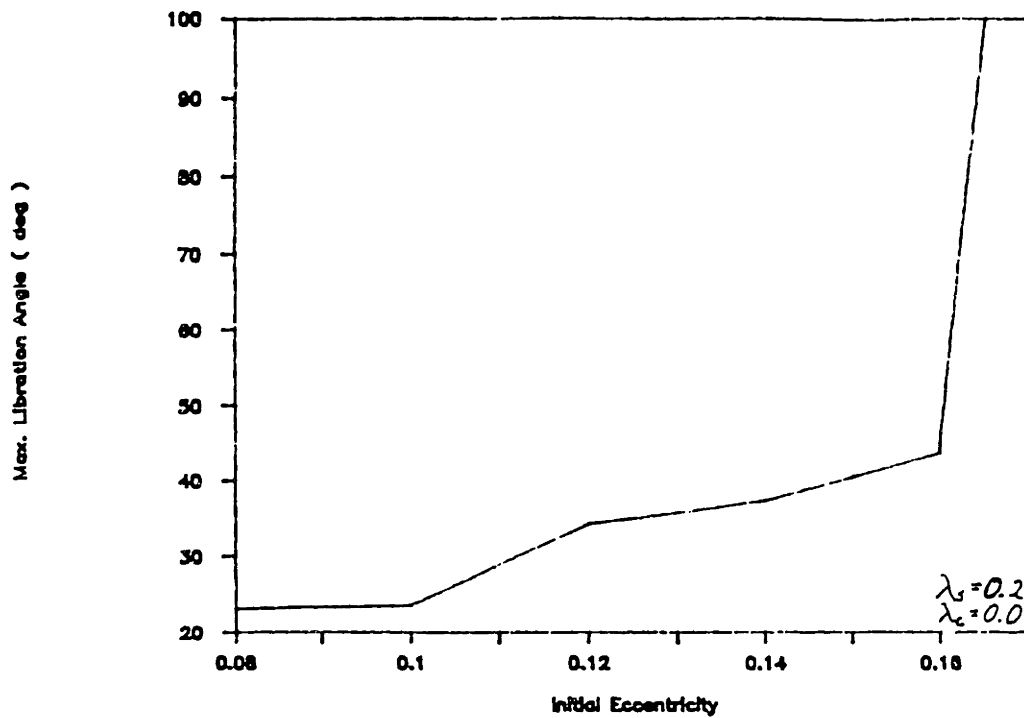


Figure 21. Max. Lib. Angle vs. Init. Eccentricity

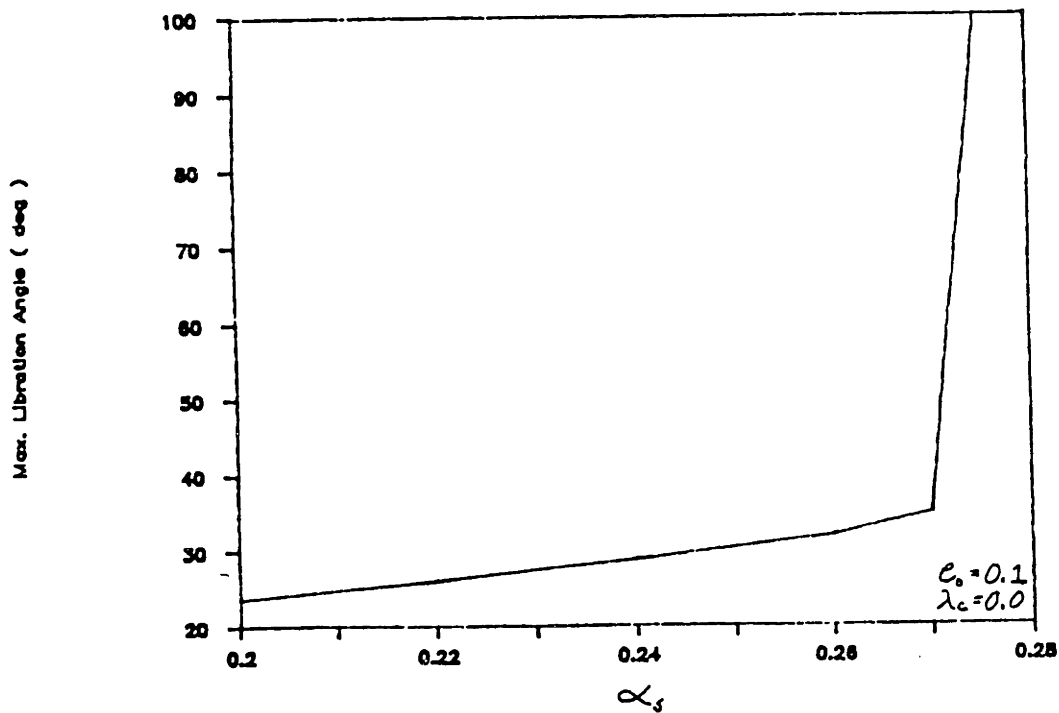


Figure 22. Max. Lib. Angle vs.  $\lambda_s$

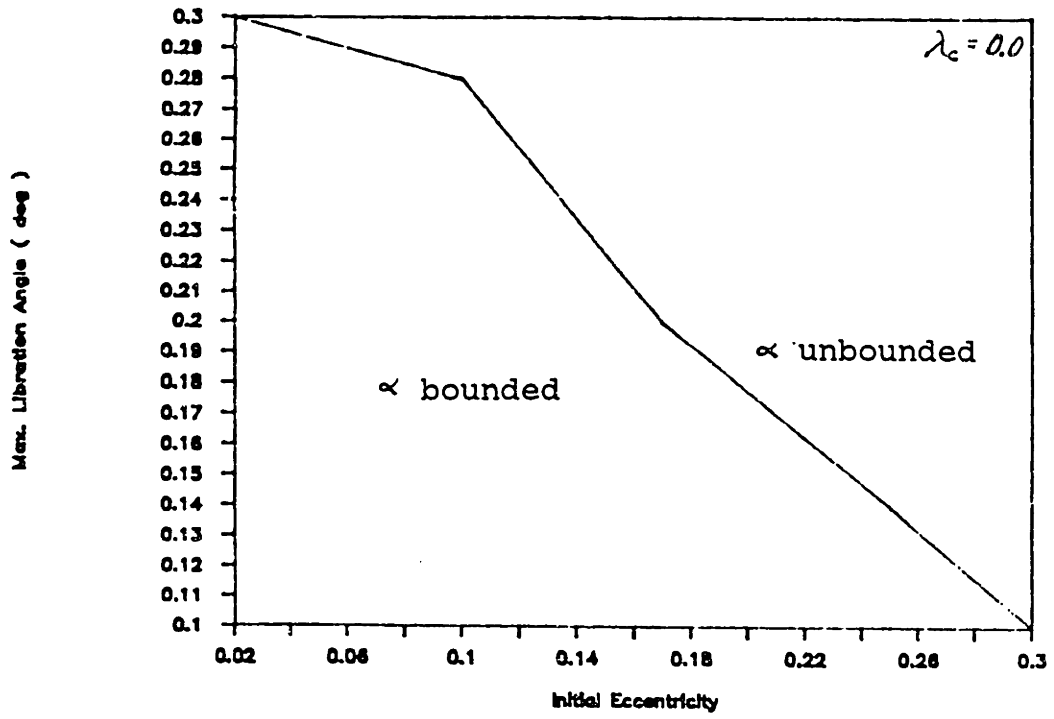


Figure 23. Max. Lib. Angle vs. Init. Eccentricity

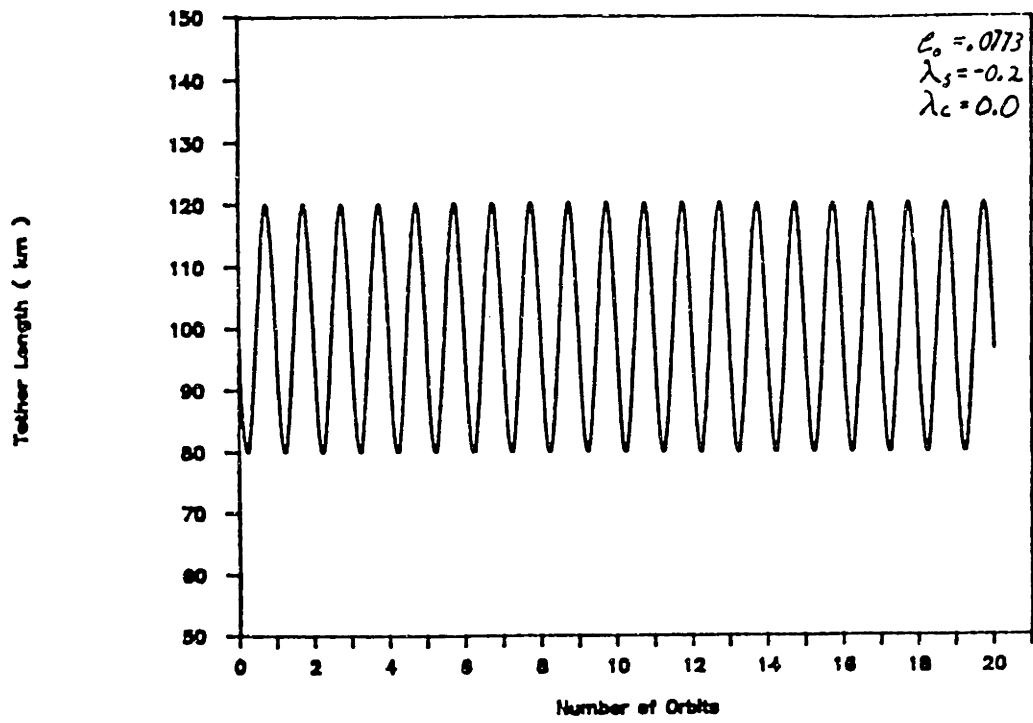


Figure 24. Tether Length vs. No. of Orbits  
Over Twenty Orbits

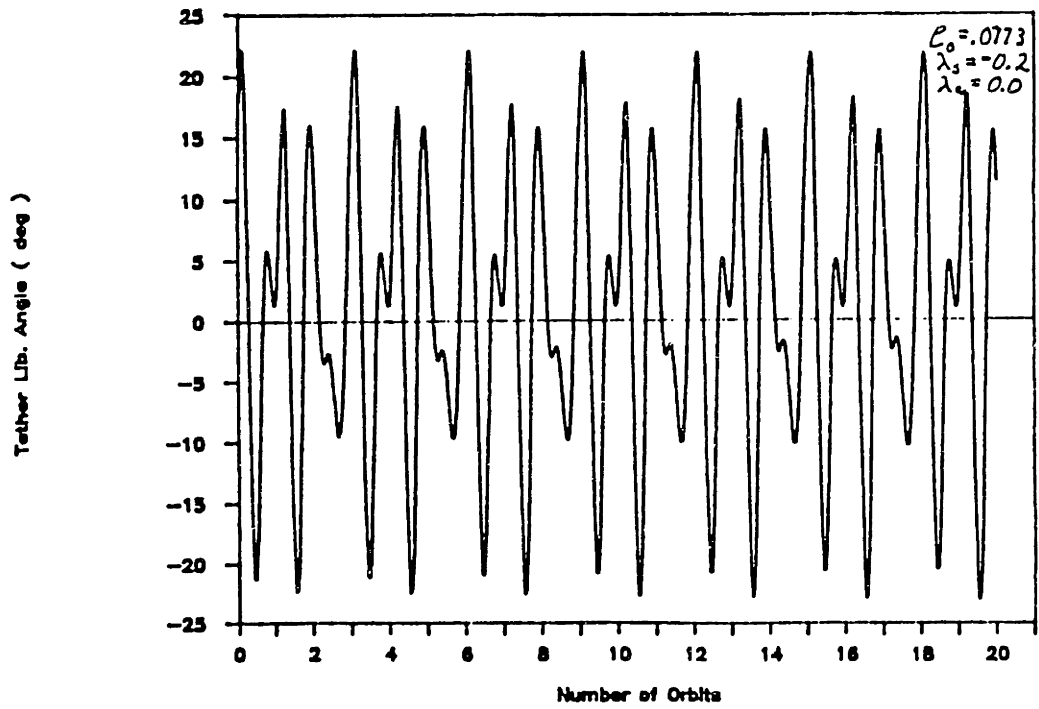


Figure 25. Tether Lib. Angle vs. No. of Orbits  
Over Twenty Orbits

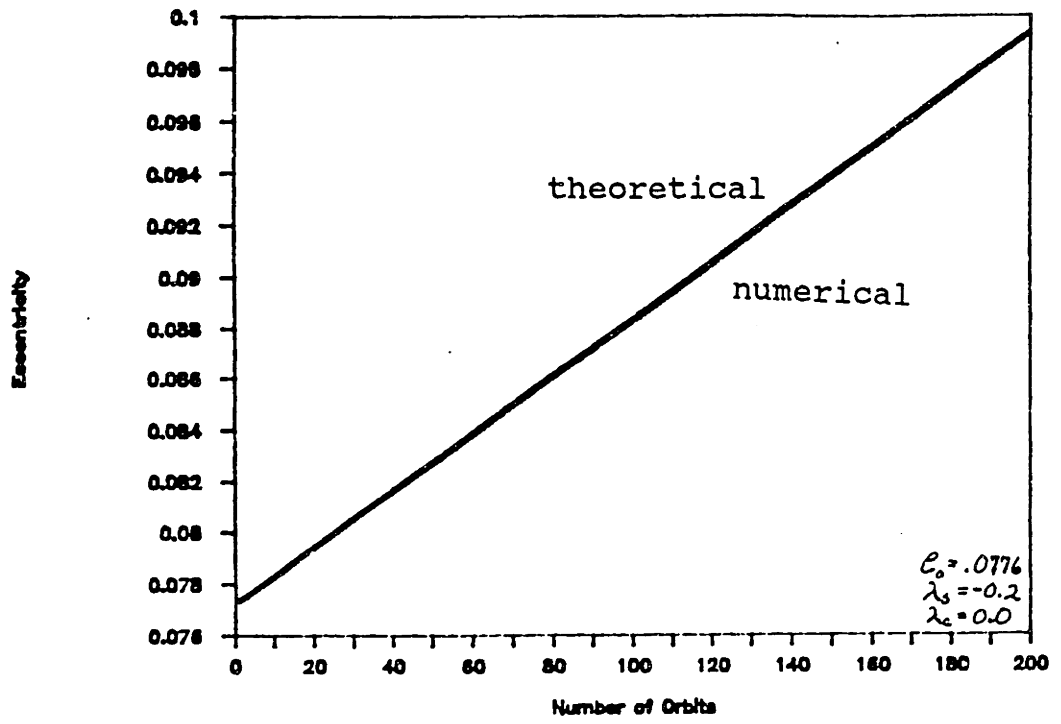


Figure 26. Eccentricities vs No. of Orbits  
Analytical and Numerical

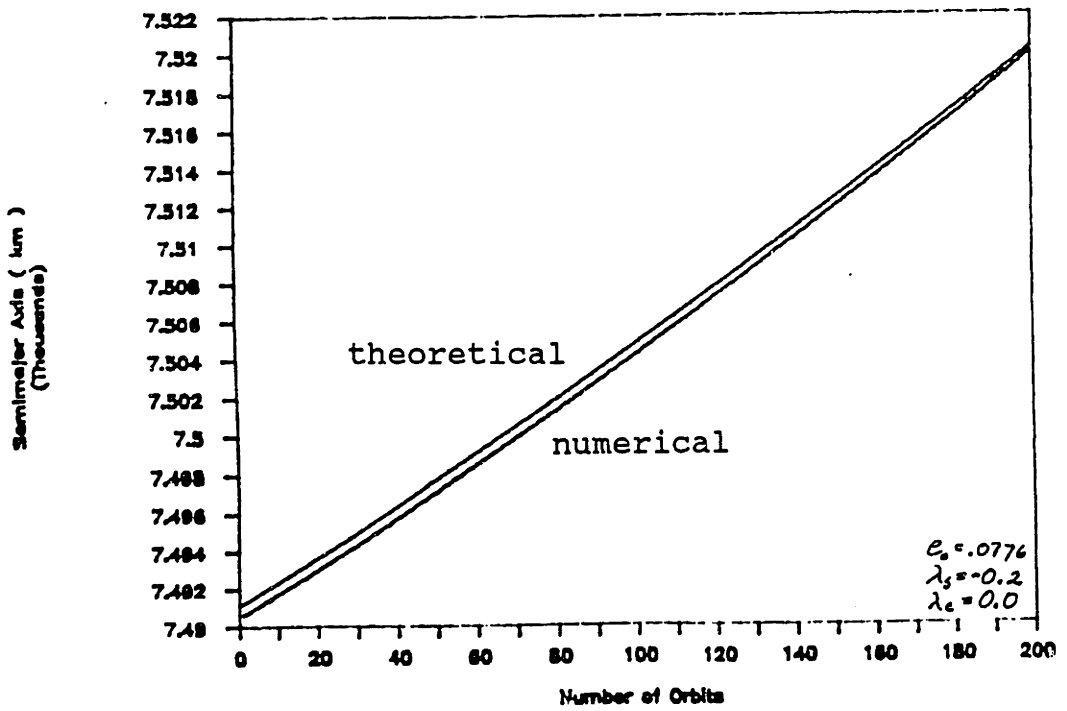


Figure 27. Semimajor Axis vs. No. of Orbits  
Analytical and Numerical

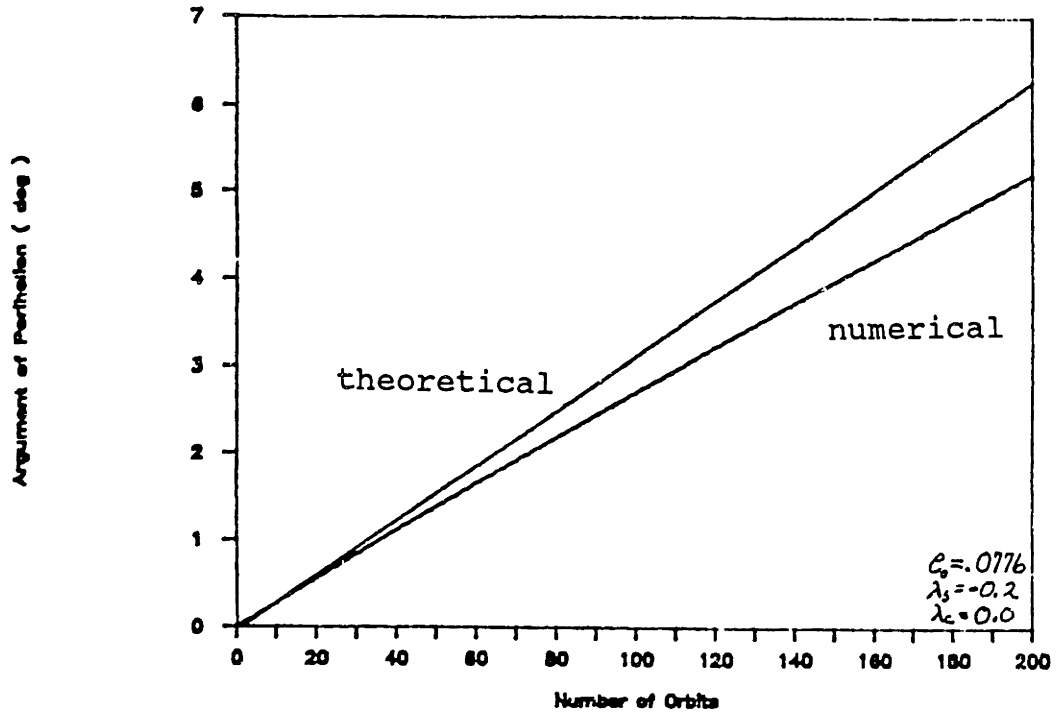


Figure 28. Arg. of Perihelion vs. No. of Orbits  
 Analytical and Numerical

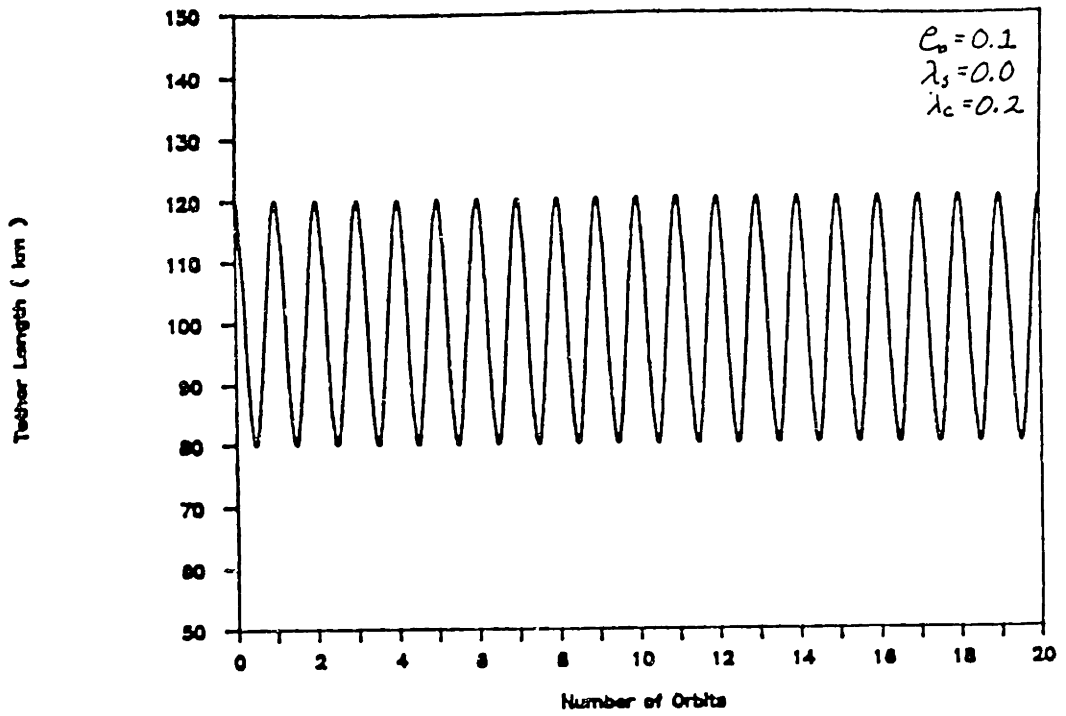


Figure 29. Tether Length vs. No. of Orbits  
Over Twenty Orbits

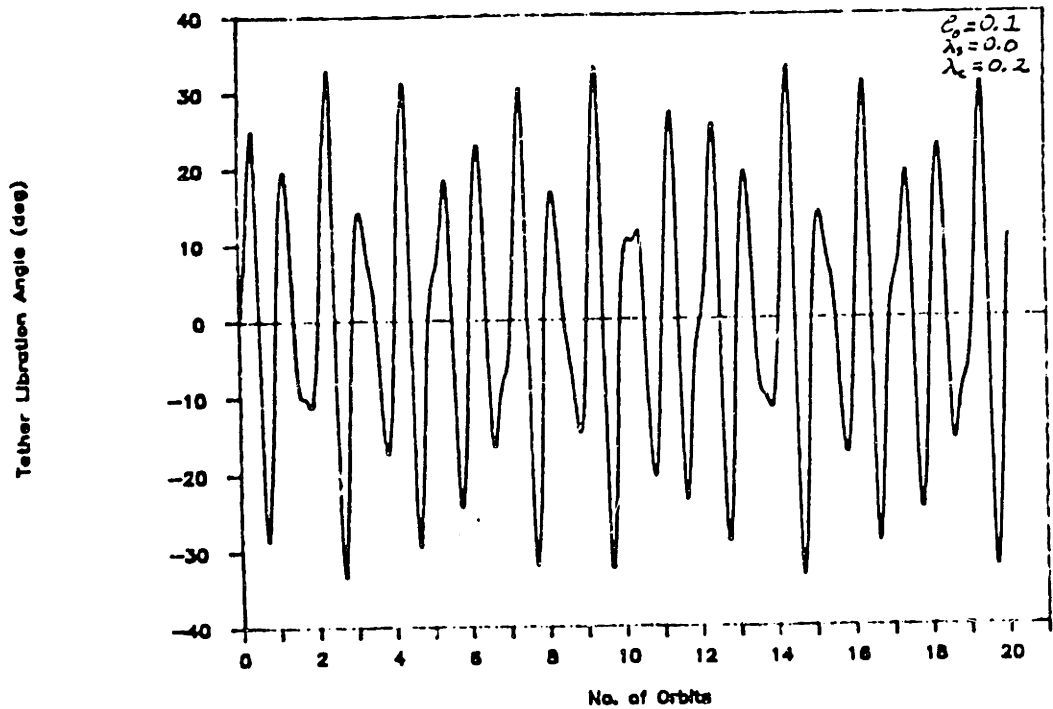


Figure 30. Tether Lib. Angle vs. No. of Orbits  
Over Twenty Orbits

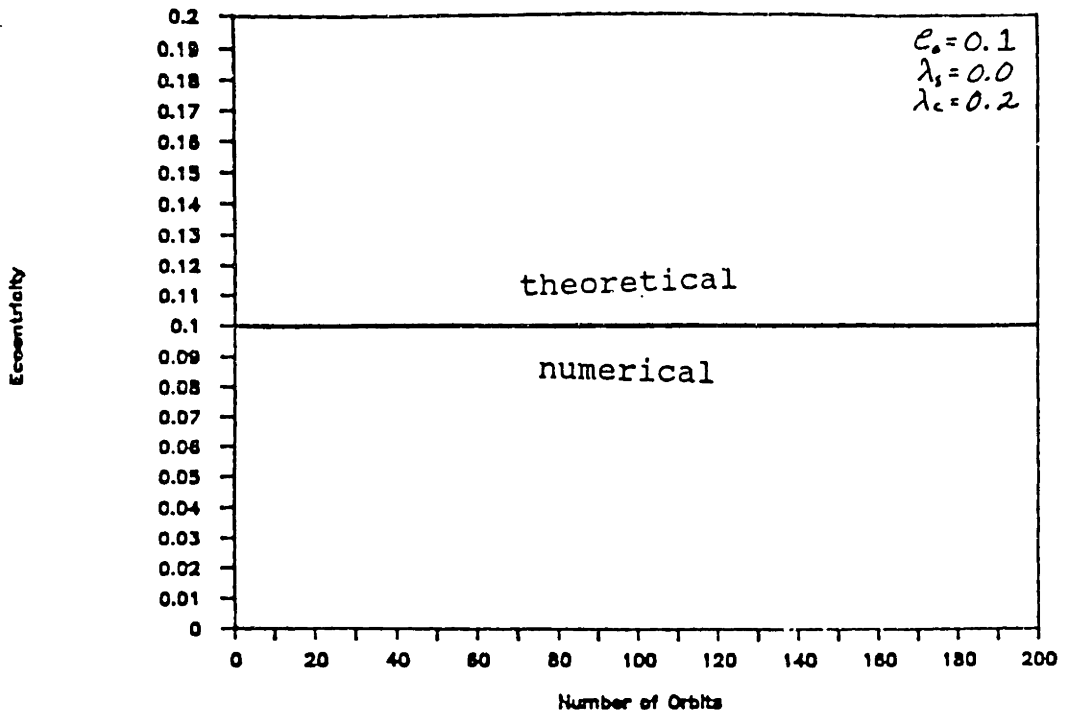


Figure 31. Eccentricities vs. No. of Orbits  
Analytical and Numerical

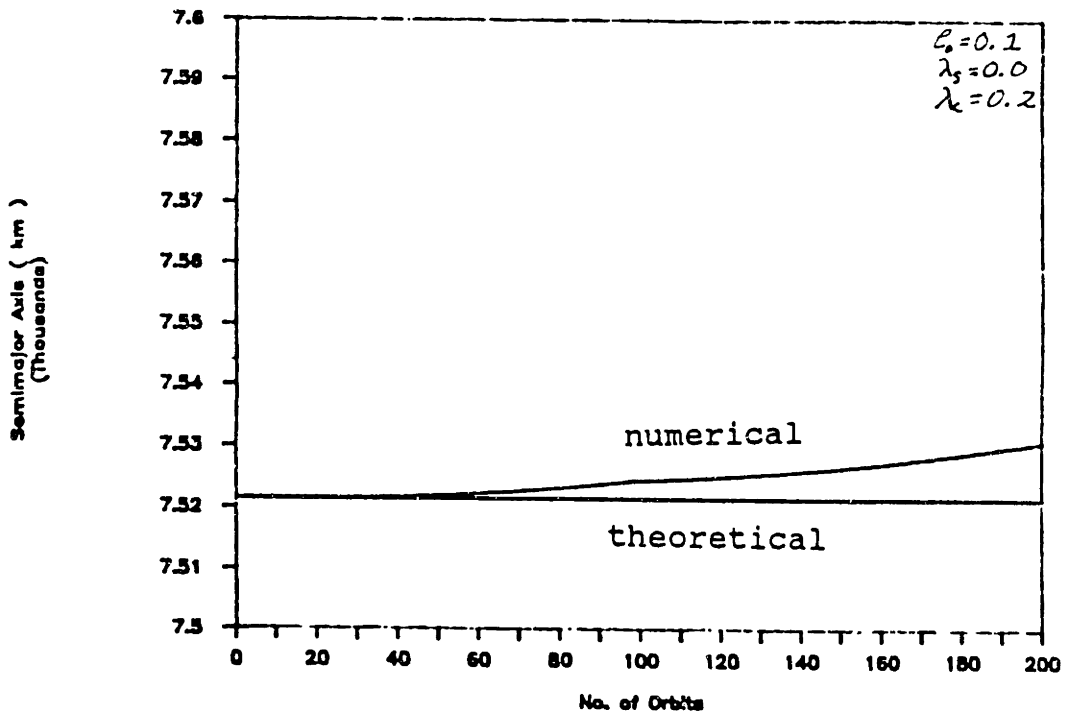


Figure 32. Semimajor Axis vs. No. of Orbits  
Analytical vs. Numerical



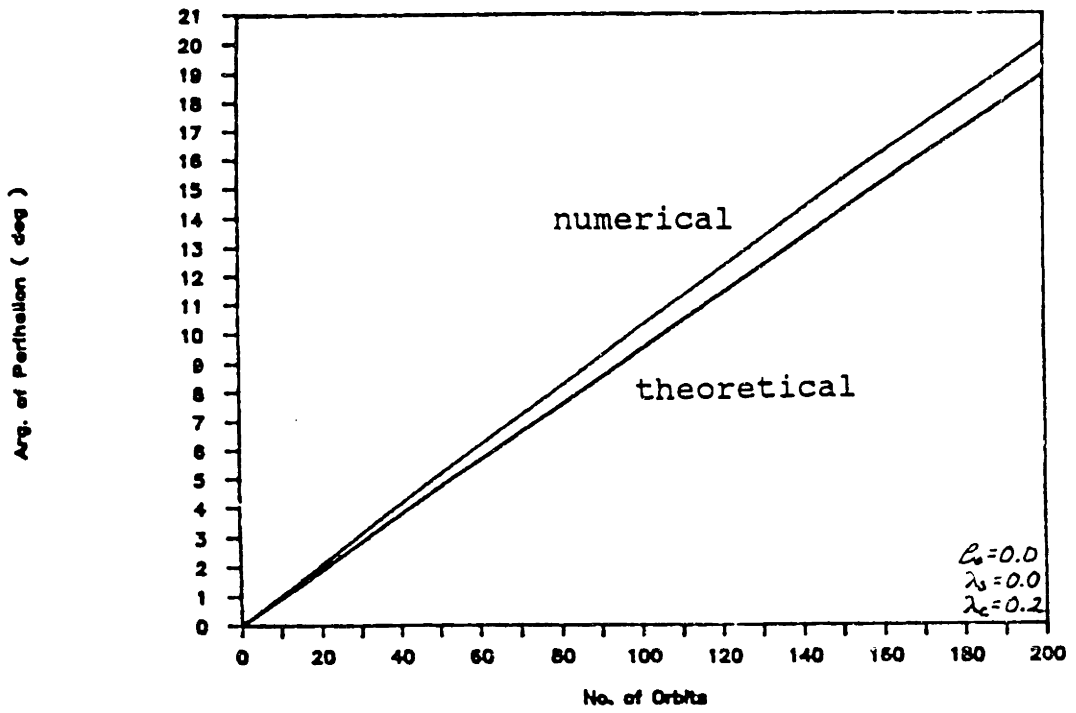


Figure 33. Arg. of Perihelion vs. No. of Orbits  
 Analytical vs. Numerical

APPENDIX A

CONSERVATION OF ANGULAR MOMENTUM FOR A DUMBBELL  
IN ORBIT ABOUT A SPHERICAL PLANET

Consider the geometry and forces action on an orbiting dumbbell, two masses connected by a tether, in Figure A1 and Figure A2. The total angular momentum of a dumbbell, may be written as follows:

$$\vec{L} = m_1 \vec{r}_1 \times \vec{v}_1 + m_2 \vec{r}_2 \times \vec{v}_2 \quad (\text{A.1})$$

Differentiating the angular momentum with respect to time, one obtains,

$$\frac{dL}{dt} = \vec{r}_1 \times m_1 \frac{d\vec{v}_1}{dt} + m_1 \frac{d\vec{r}_1}{dt} \times \vec{v}_1 + \vec{r}_2 \times m_2 \frac{d\vec{v}_2}{dt} + m_2 \frac{d\vec{r}_2}{dt} \times \vec{v}_2 \quad (\text{A.2})$$

The second and fourth terms of this equation are equal to zero since

$$\vec{v}_1 = \frac{d\vec{r}_1}{dt} \quad (\text{A.3})$$

$$\vec{v}_2 = \frac{d\vec{r}_2}{dt} \quad (\text{A.4})$$

Let  $F_{TOT}$ ,  $F_{INT}$  and  $F_{ext}$  be the total sum of the forces, the internal forces and the external forces acting on a mass respectively. Equation A.2 may then be written,

$$\begin{aligned} \frac{dL}{dt} &= \vec{r}_1 \times \vec{F}_1(TOT) + \vec{r}_2 \times \vec{F}_2(TOT) = \vec{r}_1 \times [\vec{F}_1(INT) + \vec{F}_1(EXT)] \\ &+ \vec{r}_2 \times [\vec{F}_2(INT) + \vec{F}_2(EXT)] \end{aligned} \quad (\text{A.5})$$

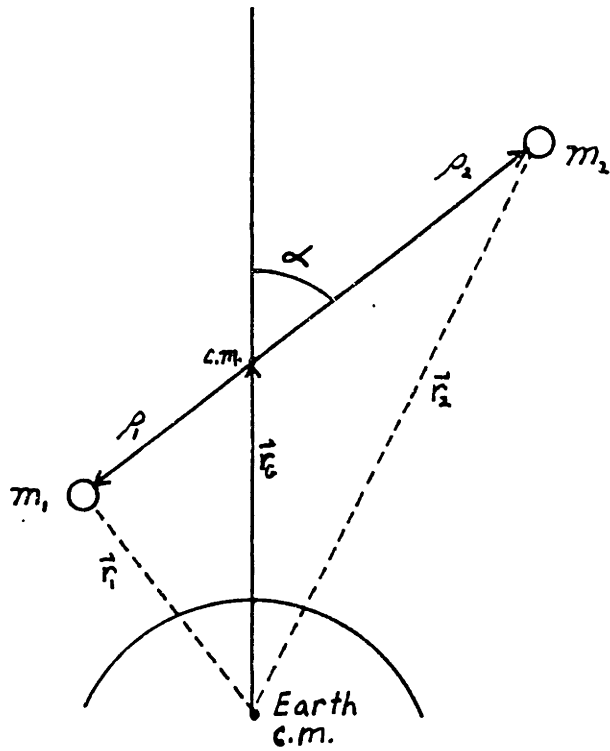


Figure A1. Geometry of an Orbiting Dumbbell

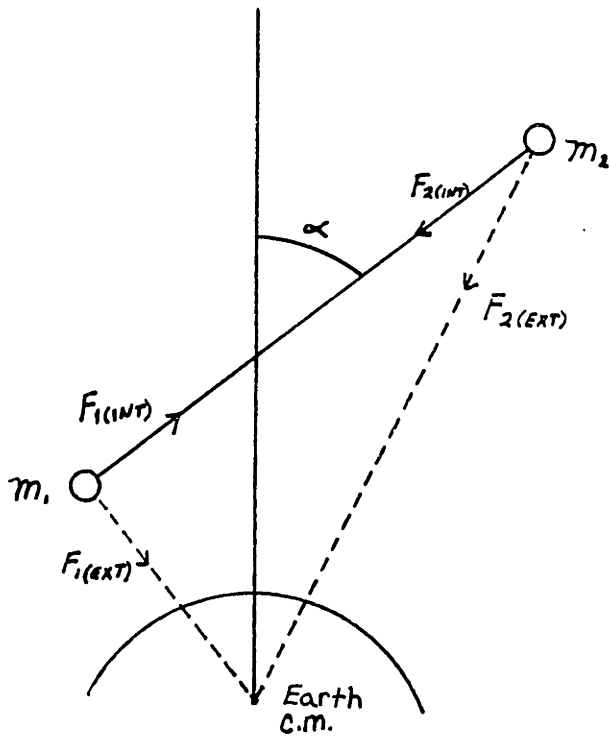


Figure A2. Forces Acting on an Orbiting Dumbbell

But the external forces are the gravity forces, and  $\vec{F}_{1(\text{EXT})}$  is aligned with  $\vec{r}_1$ , and  $\vec{F}_{2(\text{EXT})}$  is aligned with  $\vec{r}_2$ . Therefore

$$\vec{r}_1 \times \vec{F}_{1(\text{EXT})} = \vec{r}_2 \times \vec{F}_{2(\text{EXT})} = 0 \quad (\text{A.6})$$

Equation A.5 may now be written as,

$$\frac{dL}{dt} = \vec{r}_1 \times \vec{F}_{1(\text{EXT})} = \vec{r}_2 \times \vec{F}_{2(\text{EXT})} = 0 \quad (\text{A.7})$$

Let  $\vec{r}_1$  and  $\vec{r}_2$  be written in terms of the distance from the center of earth to the center of gravity of the dumbbell,  $\vec{r}_G$ , and the distance from the c.g. of the dumbbell to the two masses at the end of the tether,  $\rho_1$  and  $\rho_2$ :

$$\vec{r}_1 = \vec{r}_G + \vec{\rho}_1 \quad (\text{A.8})$$

$$\vec{r}_2 = \vec{r}_G + \vec{\rho}_2 \quad (\text{A.9})$$

Substituting into equation A.7, one obtains,

$$\begin{aligned} \frac{dL}{dt} &= (\vec{r}_G + \vec{\rho}_1) \times \vec{F}_{1(\text{INT})} + (\vec{r}_G + \vec{\rho}_2) \times \vec{F}_{2(\text{INT})} \\ &= \vec{r}_G \times (\vec{F}_{1(\text{INT})} + \vec{F}_{2(\text{INT})}) + \vec{\rho}_1 \times \vec{F}_{1(\text{INT})} + \vec{\rho}_2 \times \vec{F}_{2(\text{INT})} \end{aligned} \quad (\text{A.10})$$

The sum of the internal forces in the first term of equation 9, must be equal to zero for the system to be in equilibrium. For a dumbbell, these forces are just the tension forces in the tether which must be

equal and opposite. The second and third terms of equation A.10 must also be equal to zero since the internal tension forces are aligned along the tether and are therefore, parallel to  $\vec{p}_1$  and  $\vec{p}_2$ . Equation A.10, may be rewritten as follows,

$$\frac{dL}{dt} = 0 \tag{A.11}$$

Therefore, total angular momentum must be conserved for an orbiting dumbbell. Note: the above proof is independent of tether length. Thus, total angular momentum must still be conserved for a dumbbell whose tether length is made to vary periodically.

APPENDIX B

DERIVATION OF THE TENSION IN A LENGTH VARYING TETHER

To calculate the tension in a length varying tether, consider the free body diagram of the forces acting on one of the masses at the end of the tether, say  $m_2$ . <sup>See Figure B1.</sup> Using equations 2.8 and 2.9, the radial and tangential accelerations acting on  $m_2$  are given by,

$$\frac{(F_r)_2}{m_2} = (a_r)_2 = \frac{-\mu}{r_G^2} \left[ 1 - \frac{2y_2}{r_G} + 3 \frac{y_2^2 - 1/2 x_2^2}{r_G^2} \right] - \frac{T \cos \alpha}{m_2} \quad (B.1)$$

$$\frac{(F_\theta)_2}{m_2} = (a_\theta)_2 = \frac{-\mu}{r_G^2} \frac{x_2}{r_G} \left[ 1 - 3 \frac{y_2}{r_G} \right] - \frac{T \sin \alpha}{m_2} \quad (B.2)$$

Equations B.1 and B.2 may be combined and written in terms of the total acceleration of mass  $m_2$  as,

$$a_2 = \frac{-T}{m_2} - \frac{\mu}{r_G^2} \cos \alpha - \frac{\mu}{r_G^2} \left[ \frac{l_2}{r_G} (-2 + 3 \sin^2 \alpha) + 3 \left( \frac{l_2}{r_G} \right)^2 \cos \alpha (1 - \frac{5}{2} \sin^2 \alpha) \right] \quad (B.3)$$

where,

$$\cos \alpha = \frac{y_2}{l_2} \quad (B.4)$$

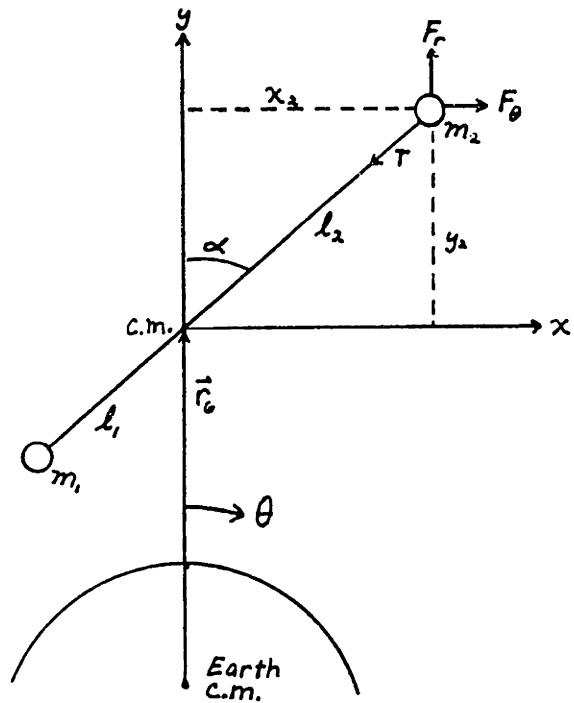


Figure B1. Geometry and Forces Acting on A Dumbbell Mass

$$\text{Sin}\alpha = \frac{x_2}{l_2} \quad (\text{B.5})$$

The total acceleration of mass  $m_2$  may also be written in terms of the center of mass, the relative, the centifical and the *Coriolis* accelerations.

$$\vec{a}_2 = \vec{a}_{\text{cm}} + \vec{a}_{m_2/\text{c.m.}} + \vec{a}_{\text{cor}} + \vec{a}_{\text{rel}} \quad (\text{B.6})$$

The center of mass acceleration is the sum of the radial and tangential center of mass accelerations which are given by the right hand sides of equations 2.18 and 2.19. The relative, centifical and *Coriolis* accelerations may be found using the following expressions for the angular velocity and distance  $l_2$ :

$$\vec{w} = -\dot{\theta}\vec{k} \quad (\text{B.7})$$

$$\vec{l}_2 = x\vec{i} + y\vec{j} \quad (\text{B.8})$$

Equation B.6 may now be written as,

$$\begin{aligned} a_r = & \frac{-\mu}{r_G^2} \text{Cos}\alpha - \frac{3\mu}{r_G^2} \frac{m_{12}}{m} \left(\frac{l}{r_G}\right)^2 \left(1 - \frac{5}{2} \text{Sin}^2\alpha\right) \text{Cos}\alpha \\ & + \ddot{l}_2 - l_2(\dot{\alpha} + \dot{\theta})^2 \end{aligned} \quad (\text{B.9})$$

The distance from mass  $m_2$  to the center of mass of the dumbbell,  $l_2$ , can be written in terms of the total tether length  $l$ , and the two masses  $m_1$  and  $m_2$ .



$$l_2 = \frac{m_1}{m_1 + m_2} l \quad (\text{B.10})$$

Using equation B.10, equations B.3 and B.9 may be equated and solved for the instantaneous tether tension.

$$\begin{aligned} T = & \frac{-\mu}{r_G^3} m_{12} l (-2 + 3 \sin^2 \alpha) \\ & - 3 \frac{\mu}{r_G^4} l^2 \cos \alpha (1 - \frac{5}{2} \sin^2 \alpha) \frac{m_{12}}{m} (m_1 - m_2) \\ & - \ddot{l} m_{12} + l m_{12} (\dot{\alpha} + \dot{\theta})^2 \end{aligned} \quad (\text{B.11})$$

# APPENDIX C: NUMERICAL ANALYSIS PROGRAM

## PROGRAM NOTATION

THE = MAIN PROGRAM  
 SIS = SUBROUTINE, CALCULATES RUNGE KUTTA VALUES  
 CON = SUBROUTINE, CALCULATES LIBRATION ANGLE INITIAL CONDITIONS (CONSTANTS AND PHASE ANGLES).  
 INHY = SUBROUTINE, CALCULATES THE INVERSE HYPERBOLIC TANGENT.

A = SEMIMAJOR AXIS (KM).  
 AC = CONSTANT OF COSINE TERM IN TETHER LENGTH EQUATION.  
 AL = TETHER LIBRATION ANGLE (RADIAN).  
 ALD = TETHER LIBRATION ANGLE (DEGREES).  
 AMX = MAXIMUM TETHER LIBRATION ANGLE IN ORBIT COMPLETED (RADIAN).  
 AMXD = MAXIMUM TETHER LIBRATION ANGLE IN ORBIT COMPLETED (DEGREES).  
 AR = DERIVATIVE OF THE ORBITAL RADIUS WITH RESPECT TO TIME (KM/SEC).  
 ARF = "AR" AT LAST RUNGE KUTTA ITERATION (KM/SEC).  
 AS = CONSTANT OF SINE TERM IN TETHER LENGTH EQUATION.  
 ATH = SEMIMAJOR AXIS THEORETICAL VALUE (KM)  
 DA = DERIVATIVE OF "AL" WITH RESPECT TO TIME (RADIAN).  
 DAD = DERIVATIVE OF "AL" WITH RESPECT TO TIME (DEGREES).  
 DATH = DERIVATIVE OF THE TETHER LIBRATION ANGLE WITH RESPECT TO THETA AT T=0.0 (RADIAN).  
 DL = DERIVATIVE OF THE TETHER LENGTH WITH RESPECT TO TIME (KM/SEC)  
 DDL = SECOND DERIVATIVE OF THE TETHER LENGTH WITH RESPECT TO TIME (KM/SEC).  
 DT = DERIVATIVE OF THETA WITH RESPECT TO TIME (RADIAN/SEC).  
 DTA = DERIVATIVE OF THE LIBRATION ANGLE WITH RESPECT TO TIME AT T=0.0 (RADIAN/SEC).  
 ECC = ECCENTRICITY.  
 ECCO = ECCENTRICITY AT T=0.0.  
 ECTH = THEORETICAL ECCENTRICITY VALUE.  
 GR = EARTH GRAVITATIONAL CONSTANT (KM\*\*3.0/SEC\*\*2.0)  
 H = RUNGE KUTTA STEP SIZE (RADIAN).  
 HD = RUNGE KUTTA STEP SIZE (DEGREES).  
 L = ANGULAR MOMENTUM OF THE CENTER OF MASS (KM\*\*2.0/SEC)  
 LPM = TOTAL ANGULAR MOMENTUM  
 M1 = MASS AT END OF TETHER, NEAREST EARTH (KG).  
 M2 = MASS AT END OF TETHER, FARTHEST FROM EARTH (KG).  
 ORC = NUMBER OF ORBITS COMPLETED.  
 PAR = ORBITAL PARAMETER.  
 PER = ORBITAL PERIOD (SEC).  
 PERH = ORBITAL PERIOD (HOURS).  
 PERHO = ORBITAL PERIOD AT LAST RUNGE KUTTA ITERATION (HOURS).  
 POW = POWER REQUIRED FOR REELING OPERATION (WATTS)  
 POWK = POWER REQUIRED FOR REELING OPERATION (KWATTS).  
 POWX = MAXIMUM POWER REQUIRED FOR REELING OPERATION IN LAST ORBIT COMPLETED.  
 R = TETHER LENGTH (KM).  
 RA = APOGEE RADIUS (KM).  
 RB = MEAN TETHER LENGTH (KM)  
 RF = ORBITAL RADIUS AT LAST RUNGE KUTTA ITERATION (KM).  
 RG = ORBITAL RADIUS (CENTER OF EARTH TO CENTER OF MASS)  
 RP = PERIGEE RADIUS  
 TEN = TETHER TENSION (NEWTONS/1000.0)  
 TENN = TETHER TENSION (NEWTONS).  
 TH = TRUE ANOMOLY (RADIAN).  
 THD = TRUE ANOMOLY (DEGREES).  
 THF = "THD" AT LAST RUNGE KUTTA ITERATION (DEGREES).  
 TIMH = TETHER OPERATION TIME (HOURS).  
 WD = ARGUMENT OF PERIHELION (DEGREES).  
 WLD = ARGUMENT OF PERIHELION LINEARIZED THEORETICAL VALUE (DEGREES).  
 WTH = ARGUMENT OF PERIHELION THEORETICAL VALUE (RADIAN).  
 WTHD = ARGUMENT OF PERIHELION THEORETICAL VALUE (DEGREES).

# MAIN PROGRAM

	IMPLICIT REAL*16 (A-H, K-Z)	THE00010
C	COMMON /ALL/ K(4), N(4), P(4), Q(4),	THE00020
	& H, LPM, GR, MR, R, M12,	THE00030
	& RGT, LT, ART, ALT,	THE00040
	& ECC, TH, AS, AC,	THE00050
	& C1, C8, P1, P8, RR, QR, I	THE00060
C	SET INITIAL CONDITIONS.	THE00070
C	ECC = .10 DO	THE00080
	ECCO = ECC	THE00090
	TH = 0.0 DO	THE00100
	THD = 0.0 DO	THE00110
	AC = 0.0 DO	THE00120
	AS = 0.2 DO	THE00130
	CALL CON	THE00140
	RP = 6770.0 DO	THE00150
C	A = 7491.36115 DO	THE00160
C	RP = A*(1.0 - ECC)	THE00170
	A = RP/(1.0-ECC)	THE00180
	RA = A * (1.0+ECC)	THE00190
	PAR = A * (1.0 - ECC**2.0)	THE00200
	RG = RP	THE00210
	GR = 398778.0 DO	THE00220
	RB = 100.0 DO	THE00230
	R = RB * (1.0 + AC*COS(TH) + AS*SIN(TH))	THE00240
	PER = (6.283185308 DO) * SQRT(A**3.0/GR)	THE00250
	PERHO = PER/3600.0	THE00260
	ORC = 0.0	THE00270
	SIGN = 1.0	THE00280
	X = 0.0	THE00290
	X10 = 10.0	THE00300
	X1 = 1.0	THE00310
	M1 = 100000.0	THE00320
	M2 = 10000.0	THE00330
	M = M1 + M2	THE00340
	MM = M1 - M2	THE00350
	M12 = (M1*M2)/M	THE00360
	MR = M12/M	THE00370
	LPM = SQRT(GR*PAR)	THE00380
	MS3 = SQRT(3.0)	THE00390
	AL = (4.0/MS3) * (C1*COS(P1) + C8*COS(P8))	THE00400
	AMX = AL	THE00410
	DATH = (4.0/MS3) * (0.0 - C1*SIN(P1) - MS3*C8*SIN(P8))	THE00420
	DT = (LPM/RG**2.0) * (1.0 - MR*((R/RG)**2.0) * (DATH + 1.0))	THE00430
	DA = DT * DATH	THE00440
	L = (RG**2.0)* DT	THE00450
	AR = (DTGD * ECC * PAR * SIN(TH))/(1.0 + ECC * COS(TH))**2.0	THE00460
C	H = .10471976 DO	THE00470
C	HD = 6.0 DO	THE00480
	H = .17453293 DO	THE00490
	HD = 10.0	THE00500
	TIMH = 0.0 DO	THE00510
	TW = SQRT(2.0)	THE00520
		THE00530
		THE00540
		THE00550

	LT = L + .5 * N(2)	THEO1110
	ART = AR + .5 * P(2)	THEO1120
	ALT = AL + .5 * Q(2)	THEO1130
	CALL SIS	THEO1140
C		THEO1150
C	FIND K4, N4, P4, Q4 :	THEO1160
C		THEO1170
	I = 4	THEO1180
	RGT = RG + K(3)	THEO1190
	LT = L + N(3)	THEO1200
	ART = AR + P(3)	THEO1210
	ALT = AL + Q(3)	THEO1220
	CALL SIS	THEO1230
C		THEO1240
C	FIND NEW VALUES FOR RG, L, AR, AL :	THEO1250
C		THEO1260
	RG = RG + (K(1) + 2*K(2) + 2*K(3) + K(4))/6.0	THEO1270
	L = L + (N(1) + 2*N(2) + 2*N(3) + N(4))/6.0	THEO1280
	AR = AR + (P(1) + 2*P(2) + 2*P(3) + P(4))/6.0	THEO1290
	AL = AL + (Q(1) + 2*Q(2) + 2*Q(3) + Q(4))/6.0	THEO1300
C		THEO1310
C	FIND AL IN DEGREES, AND THE DERIVATIVE OF AL WITH RESPECT	THEO1320
C	TO TIME.	THEO1330
C		THEO1340
	ALD = AL * (57.2957795 DO)	THEO1350
C		THEO1360
	I = 1	THEO1370
	RGT = RG	THEO1380
	LT = L	THEO1390
	ART = AR	THEO1400
	ALT = AL	THEO1410
	CALL SIS	THEO1420
	DT = L/RG**2.0	THEO1430
	DA = Q(1) * DT	THEO1440
	DAD = DA * (57.2957795)	THEO1450
C		THEO1460
C		THEO1470
C	UPDATE RA AND RP, WD, ORC, PER: NEED TO START PROGRAM AT	THEO1480
C	PERIGEE, TH = 0.0.	THEO1490
C		THEO1500
	M11= SIGN * AR	THEO1510
	IF (M11 .GE. 0.0) GO TO 180	THEO1520
	IF (AR .GE. 0.0) GO TO 170	THEO1530
	A92 = (AR-ARF)/AR	THEO1540
	RA = RG-(RG-RF)/A92	THEO1550
	SIGN = 0.0 - SIGN	THEO1560
	GO TO 180	THEO1570
170 .	A92 = (AR-ARF)/AR	THEO1580
	RP = RG-(RG-RF)/A92	THEO1590
	SIGN = 0.0 - SIGN	THEO1600
	AMX = AL	THEO1610
	ORC = ORC + 1.0	THEO1620
	TIMH = TIMH + .5*(PERH + PERHO)	THEO1630
	PERHO = PERH	THEO1640
	WD = THD-(THD-THF)/A92 - ORC*360.0	THEO1650

```

180      RF = RG
          ARF = AR
          THF = THD
C
C      FIND THE ECCENTRICITY :
          ECC = (RA-RP)/(RA+RP)
          A = .5*(RA+RP)
          PER = (6.283185308 DO) * SQRT(A**3.0/GR)
          PERH = PER/3600.0
C
C      CALCULATE THE MAXIMUM POWER REQUIRED.
          DL = RB * (AS*COS(TH) - AC*SIN(TH)) * DT
C
          D4 = -2.0*ECC*AS*COS(TH)*SIN(TH)
          D5 = 2.0*ECC*AC*SIN(TH)**2
          D6 = 0.0 - AS*SIN(TH) - AC*COS(TH)
          DDL = RB*(DT**2) * (D4+D5+D6)
C
          T4 = 0.-GR*M12*R*(0.0-2.0+3.0*SIN(AL)**2)/(RG**3)
          T5 = 0.0-3.0*GR*(R**2)*COS(AL)/(RG**4)
          T6 = SIN(AL)**2
          T66 = (1.0-2.5*T6)*MR*MM
          T7 = 0.0-DDL*M12 + R*M12*(DT+DA)**2
          TEN = T4 + T5*T66 + T7
          TENN = TEN * 1000.0
          ALF = AL
          POW = TEN*DL
          POWK = POW*1000.0
C
C      UPDATE THE MAXIMUM LIBRATION ANGLE PER ORBIT.
C      AMXD IS THE MAXIMUM LIBRATION ANGLE PER ORBIT.
C      IF ONLY PRINTING AFTER FINISHIG AN ORBIT, AMXD IS
C      THE MAXIMUM LIBRATION ANGLE THAT OCCURED IN THE LAST ORBIT.
C      LIKEWISE, POWX IS THE PEAK POWER REQUIRED PER ORBIT.
C
          M90 = ABS(AL)
          IF (M90 .LE. ABS(AMX)) GO TO 181
          AMX = AL
          AMXD = AL*(57.2957795 DO)
          AXXD = AMXD
C
          M91 = ABS(POW)
181      IF (M91 .LE. ABS(POWX)) GO TO 182
          POWX = POW
C
C      CALCULATE THE THEORETICAL VALUES.
182      N7 = 12.0*TW*PI*MR*((RB/PAR)**2)
          NN = N7 * AS
          RR = TW * ECCO
          CALL INHY
          D32 = QR - ORC*NN

```

```

THEO1660
THEO1670
THEO1680
THEO1690
THEO1700
THEO1710
THEO1720
THEO1730
THEO1740
THEO1750
THEO1760
THEO1770
THEO1780
THEO1790
THEO1800
THEO1810
THEO1820
THEO1830
THEO1840
THEO1850
THEO1860
THEO1870
THEO1880
THEO1890
THEO1900
THEO1910
THEO1920
THEO1930
THEO1940
THEO1950
THEO1960
THEO1970
THEO1980
THEO1990
THEO2000
THEO2010
THEO2020
THEO2030
THEO2040
THEO2050
THEO2060
THEO2070
THEO2080
THEO2090
THEO2100
THEO2110
THEO2120
THEO2130
THEO2140
THEO2150
THEO2160
THEO2170
THEO2180
THEO2190
THEO2200

```

```

      ECTH = (TW/2.0) * TANH(D32)
      ATH = PAR * (1.0 +.5*(TANH(D32)))**2)
C     WTH = -(ECC-ECCO + AC*LOG(ECC/ECCO))/AS
      WTHD = WTH *(57.29577951 DO)
      WL = (N7/TW) * (1.0 - 2.0*ECCO**2)*(1.0+AC/ECCO)*ORC
      WLD = WL * (57.29577951 DO)
      GO TO 190
C     WRITE (6,188) NN, RR, QR, D32
C 188 FORMAT(' NN = ', F14.6, ' RR = ', F14.6, ' QR = ', F14.6,
      &      ' D32 = ', F14.6,/)
C
C
C
C     PRINT ONLY FOR EVERY 10 ORBITS
C
C 190     C4 = ORC/X10
      IF (C4 .GE. 1.0) GO TO 200
C
      GO TO 220
C
      PRINT FOR EVERY ORBIT
C
C 190     C5 = ORC/X1
      IF (C5 .GE. 1.0) GO TO 200
      GO TO 220
C
      PRINT FOR EVERY ITERATION
C
C 190 GO TO 200
C
      PRINT THE RESULTS
C
C 200 WRITE(6,210) ORC, ECC, TH,THD, RG, AL, LPM, L, AR, TIMH, R,
      &      RA, RP, A, PERH, AMXD, ECTH, ATH, WTHD, WD, POWX,
      &      DAD
C 210 FORMAT(' ORC = ', F14.6, ' ECC = ', F14.6, ' TH = ', F14.6,/
      &      ' THD = ', F14.6, ' RG = ', F14.6, ' AL = ', F14.6,/
      &      ' LPM = ', F14.6, ' L = ', F14.6, ' AR = ', F14.6,/
      &      ' TIMH = ', F14.6, ' R = ', F14.6, ' RA = ', F14.6,/
      &      ' RP = ', F14.6, ' A = ', F14.6, ' PERH = ', F14.6,/
      &      ' AMXD = ', F14.6, ' ECTH = ', F14.6, ' ATH = ', F14.6,/
      &      ' WTHD = ', F14.6, ' WD = ', F14.6, ' POWX = ', F14.6,/
      &      ' DAD = ', F14.6,/)
C
C 211 WRITE (6,212) DL, DDL, TEN, POW
C 212 FORMAT(' DL = ', F14.6, ' DDL = ', F14.6,/
      &      ' TEN = ', F14.6, ' POW = ', F14.6,/)
C
C
C
C 200 WRITE (6,214) ORC, ECTH, ECC, WLD, WD
C 214 FORMAT( F10.1, F14.6,F14.6, F14.6, F14.6)
C
      X10=X10 + 10.0
      X1 = X1 + 1.0

```

```

THEO2210
THEO2220
THEO2230
THEO2240
THEO2250
THEO2260
THEO2270
THEO2280
THEO2290
THEO2300
THEO2310
THEO2320
THEO2330
THEO2340
THEO2350
THEO2360
THEO2370
THEO2380
THEO2390
THEO2400
THEO2410
THEO2420
THEO2430
THEO2440
THEO2450
THEO2460
THEO2470
THEO2480
THEO2490
THEO2500
THEO2510
THEO2520
THEO2530
THEO2540
THEO2550
THEO2560
THEO2570
THEO2580
THEO2590
THEO2600
THEO2610
THEO2620
THEO2630
THEO2640
THEO2650
THEO2660
THEO2670
THEO2680
THEO2690
THEO2700
THEO2710
THEO2720
THEO2730
THEO2740
THEO2750

```

	PI = 3.14159265 DO	THE00560
C		THE00570
C	PRINT INITIAL CONDITIONS:	THE00580
C		THE00590
C	80 WRITE (6,90) A, ECC, RP, RA, RG, TH, THD, AL, RB, AC, AS,	THE00600
C	& R, ORC, M1, M2; M12, PAR, LPM, L, DT, AR, PER,	THE00610
C	& H, HD	THE00620
C	90 FORMAT ( ' A = ', F12.4, ' ECC = ', F12.4, ' RP = ', F12.4, /	THE00630
C	& ' RA = ', F12.4, ' RG = ', F12.4, ' TH = ', F12.4, /	THE00640
C	& ' THD = ', F12.4, ' AL = ', F12.4, ' RB = ', F12.4, /	THE00650
C	& ' AC = ', F12.4, ' AS = ', F12.4, ' R = ', F12.4, /	THE00660
C	& ' ORC = ', F12.4, ' M1 = ', F12.4, ' M2 = ', F12.4, /	THE00670
C	& ' M12 = ', F12.4, ' PAR = ', F12.4, ' LPM = ', F12.4, /	THE00680
C	& ' L = ', F12.4, ' DT = ', F12.4, ' AR = ', F12.4, /	THE00690
C	& ' PER = ', F12.4, ' H = ', F12.4, ' HD = ', F12.4, ///)	THE00700
C		THE00710
C		THE00720
C	WRITE (6, 94)	THE00730
C	94 FORMAT ( ' AS = .2, AC = 0.0, ECCD = .1 ', /)	THE00740
C	WRITE (6,95)	THE00750
C	95 FORMAT( ' PROGRAM : ORC, ECTH, ECC, WLD, WD, ' ///)	THE00760
C	WRITE (6,96) THD, R, ALD	THE00770
C	96 FORMAT( F8.2, F14.6, F14.6)	THE00780
C		THE00790
C		THE00800
C	CALCULATE THE NEW R AND TH:	THE00810
C		THE00820
C	100 TH = TH + H	THE00830
C	THD = THD + HD	THE00840
C	R = RB * (1.0 + AC*COS(TH) + AS*SIN(TH))	THE00850
C		THE00860
C	START THE RUNGE KUTTA APPROXIMATION	THE00870
C		THE00880
C	FIND K1, N1, P1, Q1:	THE00890
C		THE00900
C	I = 1	THE00910
C	RGT = RG	THE00920
C	LT = L	THE00930
C	ART = AR	THE00940
C	ALT = AL	THE00950
C	CALL SIS	THE00960
C		THE00970
C	FIND K2, N2, P2, Q2 :	THE00980
C		THE00990
C	I = 2	THE01000
C	RGT = RG + .5 * K(1)	THE01010
C	LT = L + .5 * N(1)	THE01020
C	ART = AR + .5 * P(1)	THE01030
C	ALT = AL + .5 * Q(1)	THE01040
C	CALL SIS	THE01050
C		THE01060
C	FIND K3, N3, P3, Q3:	THE01070
C		THE01080
C	I = 3	THE01090
C	RGT = RG+.5 * K(2)	THE01100
C	IF (ORC .GE. 200.0) GO TO 250	THE02760
C	IF (ORC .EQ. 100.0) GO TO 250	THE02770
C	IF (X .GE. 2.0) GO TO 250	THE02780
C		THE02790
C	220 X = X+1.0	THE02800
C	IF (ORC .GE. 200.0) GO TO 200	THE02810
C		THE02820
C	GO TO 100	THE02830
C		THE02840
C	250 STOP	THE02850
C	END	THE02860

## SUBROUTINE SIS

	SUBROUTINE SIS	SIS00010
	IMPLICIT REAL*16 (A-H, K-Z)	SIS00020
C		SIS00030
	COMMON /ALL/ K(4), N(4), P(4), Q(4),	SIS00040
	& H, LPM, GR, MR, R, M12,	SIS00050
	& RGT, LT, ART, ALT,	SIS00060
	& ECC, TH, AS, AC,	SIS00070
	& C1, C8, P1, P8, RR, QR, I	SIS00080
C		SIS00090
	TT = (RGT**2.0)/LT	SIS00100
C		SIS00110
C	FIND THE NEW RUNGE KUTTA VALUES	SIS00120
C		SIS00130
	K(I) = H * ART * TT	SIS00140
	N(I) = (H*3.0*GR*MR/RGT)*TT* ((R/RGT)**2)* SIN(ALT) * COS(ALT)	SIS00150
	A = RGT *(ABS(LT/(RGT**2))**2 - GR/(RGT**2))	SIS00160
	B1 = (-3.0*GR*MR/(RGT**2))* ((R/RGT)**2)	SIS00170
	B2 = 1.0 - 1.5*(ABS(SIN(ALT))**2)	SIS00180
	P(I) = H * (A + B1*B2) * TT	SIS00190
	C1 = -LT/(RGT**2)	SIS00200
	C2 = -LT/(MR*R**2)	SIS00210
	D = LPM/(MR*(R**2.0))	SIS00220
	Q(I) = H * (C1+C2+D) * TT	SIS00230
C	WRITE (6,50) K(I), N(I), P(I), Q(I),	SIS00240
C	& RGT, R, LT, ART, ALT, A, B1, B2,	SIS00250
C	& C1, C2, D, TT	SIS00260
C	50 FORMAT (' K(I) = ', F14.6,	SIS00270
C	& ' N(I) = ', F14.6, ' P(I) = ', F14.6, '/' Q(I) = ',	SIS00280
C	& F14.6, ' RGT = ', F14.6, ' R = ',	SIS00290
C	& F14.6, '/' LT = ', F14.6, ' ART = ', F14.6, ' ALT = ',	SIS00300
C	& F14.6, '/' A = ', F14.6, ' B1 = ', F14.6, ' B2 = ',	SIS00310
C	& F14.6, '/' C1 = ', F14.6, ' C2 = ', F14.6, ' D = ', F14.6, /	SIS00320
C	& ' TT = ', F14.6, //)	SIS00330
C		SIS00340
	RETURN	SIS00350
	END	SIS00360

## SUBROUTINE INHY

	SUBROUTINE INHY	INH00010
	IMPLICIT REAL*16 (A-H, K-Z)	INH00020
C		INH00030
C		INH00040
	COMMON /ALL/ K(4), N(4), P(4), Q(4),	INH00050
	& H, LPM, GR, MR, R, M12,	INH00060
	& RGT, LT, ART, ALT,	INH00070
	& ECC, TH, AS, AC,	INH00080
	& C1, C8, P1, P8, RR, QR, I	INH00090
C		INH00100
	YR = (RR+1.0)/(1.0-RR)	INH00110
	QR = .5 * LOG(YR)	INH00120
C		INH00130
	RETURN	INH00140
	END	INH00150



# SUBROUTINE CON

	SUBROUTINE CON		CON00010
	IMPLICIT REAL*16 (A-H, K-Z)		CON00020
C			CON00030
	COMMON /ALL/ K(4), N(4), P(4), O(4),		CON00040
	& H, LPM, GR, MR, R, M12,		CON00050
	& RGT, LT, ART, ALT,		CON00060
	& ECC, TH, AS, AC,		CON00070
	& C1, C8, P1, P8, RR, QR, I		CON00080
C			CON00090
C			CON00100
C			CON00110
C			CON00120
	X = AS/(2.0*ECC-AC)		CON00130
	L = ATAN(X)		CON00140
C			CON00150
	IF (AS .NE. 0.0) GO TO 1		CON00160
	S1 = 1.570796327 DO		CON00170
	S2 = S1		CON00180
	S4 = S1		CON00190
	S9 = S1		CON00200
	S10 = S1		CON00210
	S13 = S1		CON00220
	S16 = S1		CON00230
	S3 = -S1		CON00240
	S5 = S3		CON00250
	S12 = S3		CON00260
	S14 = S3		CON00270
	S17 = S3		CON00280
	GO TO 2		CON00290
1	B1 = (ECC+AC)/AS		CON00300
	X = B1		CON00310
	PQ = ATAN(X)		CON00320
	S1 = PQ		CON00330
	S2 = S1		CON00340
	S10 = S1		CON00350
	S13 = S1		CON00360
	S16 = S1		CON00370
	X = -B1		CON00380
	PQ = ATAN(X)		CON00390
	S3 = PQ		CON00400
	S12 = S3		CON00410
	S14 = S3		CON00420
	S17 = S3		CON00430
C			CON00440
	B2 = AC/AS		CON00450
	X = B2		CON00460
	PQ = ATAN(X)		CON00470
	S4 = PQ		CON00480
	S9 = S4		CON00490
C			CON00500
	X = -B2		CON00510
	PQ = ATAN(X)		CON00520
	S5 = PQ		CON00530
C			CON00540
C	NOW CALCULATE THE PHI'S AND C'S SIMULTANEOUSLY.		CON00550

C		CON00560
2	HS = 8.0*SQRT((ABS(AS))**2+(ABS(2*ECC-AC))**2)	CON00570
	SK = SQRT((ECC+AC)**2 + AS**2)	CON00580
	G1 = 3.0	CON00590
	SR3 = SQRT(G1)	CON00600
	SM = SQRT (AC**2 + AS**2)	CON00610
C		CON00620
C	WRITE (6,3)	CON00630
C	3 FORMAT (' MARK 1 ',/)	CON00640
C		CON00650
C		CON00660
	AC1 = (ECC+AC)*SR3/4.0	CON00670
	BC1 = -AS*SR3/4.0	CON00680
	BB= 0.0	CON00690
	C1 = ABS((SR3*SK)/4.0)	CON00700
	C11= SQRT((ABS(AC1))**2 +( ABS(BC1))**2)	CON00710
	SIG = AC1*SIN(BB) + BC1*COS(BB)	CON00720
	IF (SIG .GT. 0.0) C1= C1	CON00730
	IF (SIG .LT. 0.0) C1 =-C1	CON00740
C		CON00750
	Y1 = 528.0 - 352.0*SR3 + HS*(20.0 - 8.0*SR3)	CON00760
	Y2 = 6336.0 - 3520.0*SR3	CON00770
	AC1 = (ECC+AC)*Y1/Y2	CON00780
	BC1 = -AS*Y1/Y2	CON00790
	BB = (SR3 - 1.0)*L	CON00800
	C2 = ABS(Y1*SK/Y2)	CON00810
	C22= SQRT((ABS(AC1))**2 + (ABS(BC1))**2)	CON00820
	SIG = AC1*SIN(BB) + BC1*COS(BB)	CON00830
	IF (SIG .GT. 0.0) C2= C2	CON00840
	IF (SIG .LT. 0.0) C2 =-C2	CON00850
C		CON00860
C	WRITE (6,4)	CON00870
C	4 FORMAT (' MARK 2 ', /)	CON00880
C		CON00890
C		CON00900
	Y1 = 528.0 + 352.0*SR3 + HS*(20.0+8.0*SR3)	CON00910
	Y2 = -6336.0 - 3520.0*SR3	CON00920
	AC1 = -(ECC+AC)*Y1/Y2	CON00930
	BC1 = -AS*Y1/Y2	CON00940
	BB = (SR3+1.0)*L	CON00950
	C3 = ABS(Y1*SK/Y2)	CON00960
	C33= SQRT(ABS(AC1)**2 + ABS(BC1)**2)	CON00970
	SIG = AC1*SIN(BB) + BC1*COS(BB)	CON00980
	IF (SIG .GT. 0.0) C3= C3	CON00990
	IF (SIG .LT. 0.0) C3 =-C3	CON01000
C		CON01010
	Y1 = -8.0 + 4.0*SR3	CON01020
	AC1 = -AC*ECC/Y1	CON01030
	BC1 =AS*ECC/Y1	CON01040
	BB = (SR3-2.0)*L	CON01050
	C4 = ABS(ECC*SM/Y1)	CON01060
	C44= SQRT((ABS(AC1))**2 + (ABS(BC1))**2)	CON01070
	SIG = AC1*SIN(BB) + BC1*COS(BB)	CON01080
	IF (SIG .GT. 0.0) C4= C4	CON01090
	IF (SIG .LT. 0.0) C4 =-C4	CON01100

C	Y1 = 8.0 + 4.0*SR3	CONO1110
	AC1 = AC*ECC/Y1	CONO1120
	BC1 = AS*ECC/Y1	CONO1130
	BB = (SR3 + 2.0)*L	CONO1140
	C5 = ABS(ECC*SM/Y1)	CONO1150
	C55= SQRT((ABS(AC1))**2 + (ABS(BC1))**2)	CONO1160
	SIG = AC1*SIN(BB) + BC1*COS(BB)	CONO1170
	IF (SIG .GT. 0.0) C5= C5	CONO1180
	IF (SIG .LT. 0.0) C5 =-C5	CONO1190
C	P1 = S1	CONO1200
	P2 =(SR3-1.0)*L + S2	CONO1210
	P3 = (SR3+1.0)*L +S3	CONO1220
	P4 = (SR3 - 2.0)*L + S4	CONO1230
	P5 = (SR3 + 2.0)*L + S5	CONO1240
	Y1 = C2*SIN(P2) + C3*SIN(P3)	CONO1250
	Y2 = C2*COS(P2) + C3*COS(P3)	CONO1260
	X = Y1/Y2	CONO1270
	PQ = ATAN(X)	CONO1280
	P6 = PQ	CONO1290
	Y1 = C4*SIN(P4) + C5*SIN(P5)	CONO1300
	Y2 = C4*COS(P4) + C5*COS(P5)	CONO1310
	X = Y1/Y2	CONO1320
	PQ = ATAN(X)	CONO1330
	P7 = PQ	CONO1340
C	C6 = SQRT((ABS(C2))**2 + (ABS(C3))**2 + 2.0*C2*C3*COS(P2-P3))	CONO1350
	SIG = C2*COS(P2) + C3*COS(P3)	CONO1360
	IF (SIG .GT. 0.0) C6= C6	CONO1370
	IF (SIG .LT. 0.0) C6 =-C6	CONO1380
C	C7 = SQRT((ABS(C4))**2 + (ABS(C5))**2 + 2.0*C4*C5*COS(P4-P5))	CONO1390
	SIG = C4*COS(P4) + C5*COS(P5)	CONO1400
	IF (SIG .GT. 0.0) C7= C7	CONO1410
	IF (SIG .LT. 0.0) C7 =-C7	CONO1420
C	C8 = SQRT((ABS(C6))**2 + (ABS(C7))**2 + 2.0*C6*C7*COS(P6-P7))	CONO1430
	SIG = C6 * COS(P6) + C7*COS(P7)	CONO1440
	IF (SIG .GT. 0.0) C8= C8	CONO1450
C	Y1 = C6*SIN(P6) + C7*SIN(P7)	CONO1460
	Y2 = C6*COS(P6) + C7*COS(P7)	CONO1470
	X = Y1/Y2	CONO1480
	PQ = ATAN(X)	CONO1490
	P8 = PQ	CONO1500
C	WRITE (6, 200) S1, S3, S4, S5, P1, P2, P3, P4, P5, P6, P7, P8	CONO1510
C		CONO1520
C	200 FORMAT ( ' S1 = ', F14.8, ' S3 = ', F14.8, ' S4 = ', F14.8, /	CONO1530
C	& ' S5 = ', F14.8, ' P1 = ', F14.8, ' P2 = ', F14.8, /	CONO1540
C	& ' P3 = ', F14.8, ' P4 = ', F14.8, ' P5 = ', F14.8, /	CONO1550
C	& ' P6 = ', F14.8, ' P7 = ', F14.8, ' P8 = ', F14.8, //)	CONO1560
C		CONO1570
C	WRITE (6,300) C1, C2, C3, C4, C5, C6, C7, C8	CONO1580
C		CONO1590
C	300 FORMAT ( ' C1 = ', F14.8, ' C2 = ', F14.8, ' C3 = ', F14.8, /	CONO1600
C	& ' C4 = ', F14.8, ' C5 = ', F14.8, ' C6 = ', F14.8, /	CONO1610
C	& ' C7 = ', F14.8, ' C8 = ', F14.8, //)	CONO1620
C		CONO1630
C	RETURN	CONO1640
	END	CONO1650
		CONO1660
		CONO1670
		CONO1680
		CONO1690
		CONO1700
		CONO1710
		CONO1720